AD-A091 903 UNITED TECHNOLOGIES RESEARCH CENTER EAST HARTFORD CONN F/G 20/5
INVESTIGATION OF PLASMA PROCESSES IN ELECTRONIC TRANSITION LASE--ETC(U)
NOV 80 W L NIGHAN N00014-76-C-0847
UNCLASSIFIED UTRC/R80-922617-5

END
DATE FILMED
1 81
DTIC

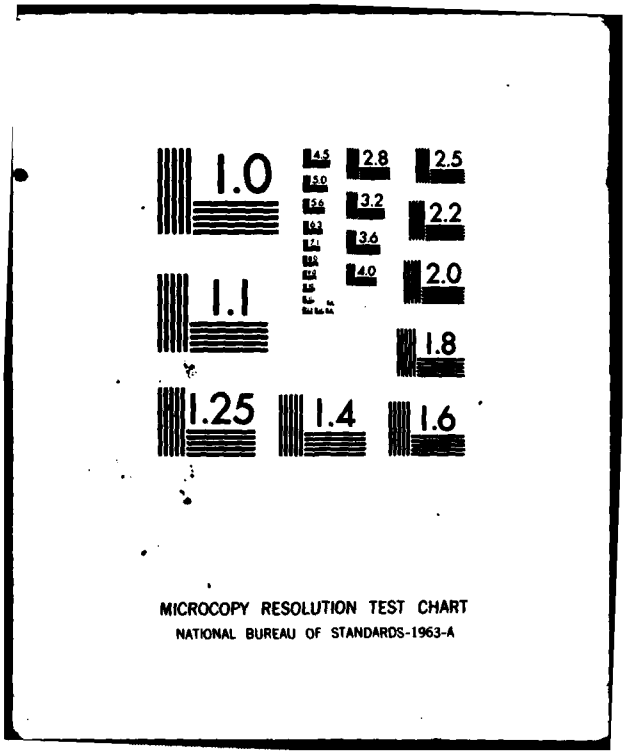
1.0
1.1
1.25
1.4
1.6
1.8
2.0
2.2
2.5
2.8
3.2
3.6
4.0
4.5
5.0
5.6
6.3
7.1
8.0
9.0
MICROCOPY RESOLUTION TEST CHART
NATIONAL BUREAU OF STANDARDS-1963-A

(12)

R80-922617-5

INVESTIGATION OF PLASMA PROCESSES IN ELECTRONIC TRANSITION LASERS

William L. Nighan

Technical Report
November 1, 1980

Sponsored by the Office of Naval Research
under Contract N00014-76-C-0847

United Technologies Research Center
East Hartford, Connecticut 06108

(9) Technical rept. 1 Nov 79 - 1 Nov 80

SECURITY CLASSIFICATION OF THIS PAGE (When Data Entered)

REPORT DOCUMENTATION PAGE	READ INSTRUCTIONS BEFORE COMPLETING FORM
1. REPORT NUMBER: R80-922617-5 ✓	2. GOVT ACCESSION NO.: AD-A092 903
4. TITLE (and Subtitle): Investigation of Plasma Processes in Electronic Transition Lasers (6)	5. TYPE OF REPORT & PERIOD COVERED: Technical Report, Nov. 1, 1979 - Nov. 1, 1980
	6. PERFORMING ORG. REPORT NUMBER: R80-922617-5 (14) UTRC
7. AUTHOR(s): (10) William L. Nighan	8. CONTRACT OR GRANT NUMBER(s): (15) N00014-76-C-0847
9. PERFORMING ORGANIZATION NAME AND ADDRESS: United Technologies Research Center ✓, Silver Lane, East Hartford, CT. 06108	10. PROGRAM ELEMENT, PROJECT, TASK AREA & WORK UNIT NUMBERS: (11) 1 Nov 80
11. CONTROLLING OFFICE NAME AND ADDRESS: (12) 78	12. REPORT DATE: November 1, 1980
	13. NUMBER OF PAGES: 78
14. MONITORING AGENCY NAME & ADDRESS (if different from Controlling Office)	15. SECURITY CLASS. (of this report): Unclassified
	15a. DECLASSIFICATION/DOWNGRADING SCHEDULE

16. DISTRIBUTION STATEMENT (of this Report)

Approved for public release; distribution unlimited. Reproduction in whole or in part if permitted for any purpose of the United States Government.

17. DISTRIBUTION STATEMENT (of the abstract entered in Block 20, if different from Report)

18. SUPPLEMENTARY NOTES

To be published in Applied Atomic Collision Physics: Gas Laser Physics (H.S.W. Massey, E. W. McDaniel and B. Bederson, eds.), Academic Press, New York, 1981.

19. KEY WORDS (Continue on reverse side if necessary and identify by block number)

Excimer lasers, Xenon-Chloride lasers, Mercury-Bromide lasers, Electron-beam controlled laser discharges, HCl vibrational excitation, HCl attachment, $HgBr_2$ ionization, $HgBr_2$ attachment, Blue-green lasers, Kinetic-processes in XeCl and HgBr lasrs.

20. ABSTRACT (Continue on reverse side if necessary and identify by block number)

This report describes the essential features of electron-beam controlled discharges of the type common to rare gas halide and mercury-halide lasers. Particular attention is directed toward the XeCl (308 nm) laser using HCl as the halogen donor, and the HgBr(502 nm) laser using $HgBr_2$. The basic kinetic processes controlling the behavior of these lasers are discussed, with special emphasis on electron collisions with HCl and $HgBr_2$, respectively.

DD FORM 1 JAN 73 1473 EDITION OF 1 NOV 65 IS OBSOLETE
S/N 0102-LF-014-6601

Unclassified
SECURITY CLASSIFICATION OF THIS PAGE (When Data Entered)

409252

PREFACE

Under the present ONR Contract, United Technologies Research Center is conducting an analytical investigation of plasma processes in electrically excited electronic transition lasers. Particular emphasis in this investigation is directed toward the two laser candidates exhibiting the most potential for development as efficient optical sources in the blue/green region of the spectrum: the 502 nm $HgBr(B)/HgBr_2$ dissociation laser, and the 308 nm XeCl laser (to be wavelength shifted to the blue/green region). A primary objective of this research is identification of fundamental mechanisms influencing laser and plasma processes. This work is being carried out in close coordination with other Corporate and Navy sponsored experimental and theoretical programs.

The present technical report is based upon a chapter to be included in "Applied Atomic Collision Physics: Gas Lasers" (H.S.W. Massey, E. W. McDaniel and B. Bederson, eds.), to be published by Academic Press. Reprints of recently published papers are also included in an appendix.

TABLE OF CONTENTS

I. INTRODUCTION

Electrically excited rare gas-halide lasers and their closely related mercury-halide counterparts are leading candidates for the development of efficient, high energy optical sources in the UV and visible regions of the spectrum (Rokni and Jacob, et al, 1981; and Parks, 1981). The plasma medium typical of these lasers is created in a near atmospheric pressure gas mixture containing a small (< 1%) fractional concentration of a halogen bearing molecule. Pulsed electrical excitation is provided by either a fast-pulse (< 100nsec duration), avalanche-type electric discharge, a beam of high intensity relativistic electrons, or an electron-beam stabilized electric discharge (Brau, 1979). In this chapter attention is focused on the latter excitation method; i.e., e-beam stabilized laser discharges, with particular emphasis on the properties of the ionized medium so created.

Electron-beam controlled discharge excitation provides selective (i.e., efficient) excitation of the working species, along with a degree of scalability which is not typical of avalanche discharges. In addition, there results a significant reduction in the technology problems often encountered when pure electron-beam pumping is utilized. Moreover, the e-beam controlled discharge excitation method is capable of generating high pressure, collision dominated glow discharges having exceptional diagnostic value. Thus, such discharges provide a rich source of fundamental information difficult to obtain by other means. In Section II of this chapter the essential features of e-beam controlled discharges of the type common to rare gas and mercury-

halide lasers are outlined. In addition, certain constraining factors which determine the range of accessible parameter space are considered in general terms as a prelude to more detailed discussion of the application of e-beam controlled discharges to xenon-chloride and mercury-bromide laser excitation.

Of the several rare gas and mercury-halide lasers under investigation, the XeCl($B \rightarrow X$) laser operating at 308 nm and the HgBr($B \rightarrow X$) laser at 502 nm have demonstrated unusual potential for a variety of applications. These lasers also represent excellent contrasting examples of lasers excited in e-beam controlled discharges. The general characteristics of these lasers are presented in Section III along with a discussion of several unique features which set the XeCl and HgBr laser apart from others in this class. Since a primary purpose of this contribution is to elucidate the characteristics of the plasma medium typical of optimum laser performance, the dominant excited state and ionic processes occurring in XeCl and HgBr laser discharges are discussed in detail in Section IV. Particular emphasis is placed on analysis of the factors influencing the concentrations of excited and ionic species, and their influence on laser/discharge properties. The accompanying discussion is presented within a framework intended to show the great progress that has been recently made in the understanding of the high pressure glow discharges common to electronic transition lasers, while at the same time indicating those areas requiring improvement in both basic data and understanding.

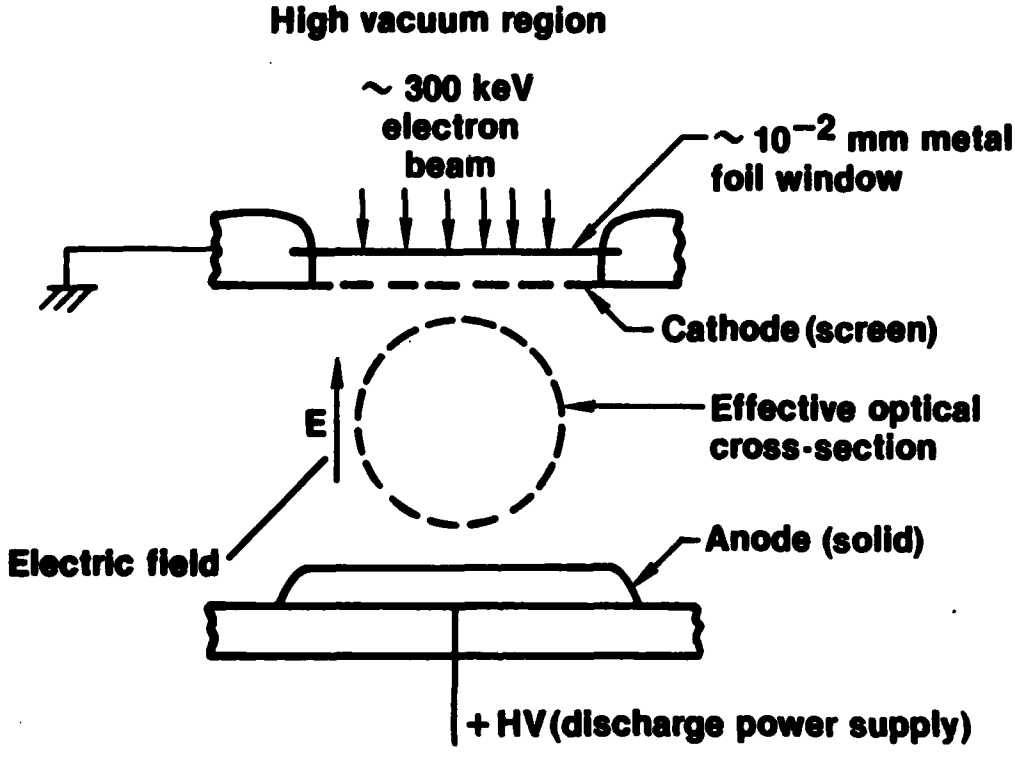

Figure 1. Schematic illustration of the experimental arrangement common to e-beam controlled laser discharges. The cross-sectional area of the discharge region is typically in the 1-100 cm^2 range and the discharge length in the optical direction is typically on the order of one meter, dimensions corresponding to active volumes in the 0.1 - 10.0 liter range.

II. ELECTRON-BEAM CONTROLLED DISCHARGES

The electron-beam controlled* discharge technique was first devised and implemented about a decade ago as a means to overcome thermal instability in large volume, high energy CO_2 laser discharges. A comprehensive article on this subject by Daugherty (1976) provides a particularly informative survey of the background and early research leading to the successful development of the first high pressure, e-beam ionized glow discharges. Figure 1 illustrates the general features of the experimental arrangement common to such discharges. Ideally, ionization of the laser gas mixture is provided by uniform irradiation of the active volume by a large-area electron-beam. The physics of the resulting ionization/excitation process has been studied extensively in recent years as described by Jacob (1981), and by Elliott and Greene (1976). Generally, such an e-beam produced plasma has an electron temperature well below that required for regenerative or self-sustained ionization. The electron temperature is elevated to the level required for efficient excitation of the medium by application of a uniform electric field as indicated in Fig. 1. When the electron temperature needed for

---

* The terms "electron-beam controlled discharge", "electron-beam sustained discharge", and "e-beam ionizer-sustainer discharge" are used interchangeably throughout the literature to describe discharges for which the e-beam is used as a source of ionization for an electric discharge having an electric-field below that required for avalanching or self-sustained operation.

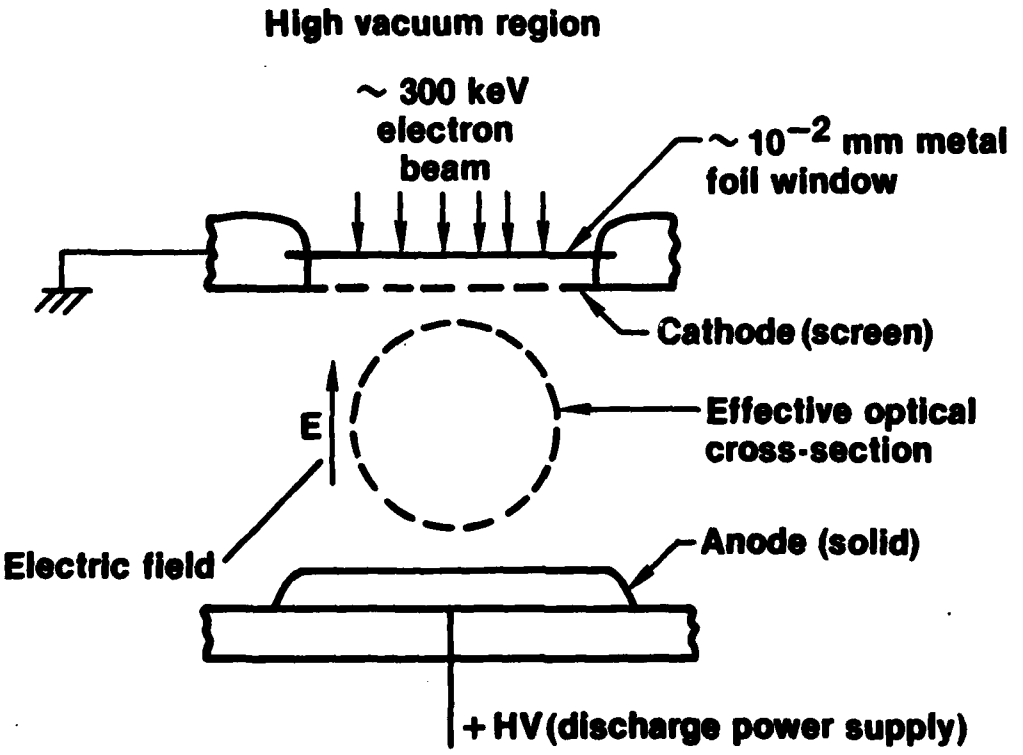

Figure 1. Schematic illustration of the experimental arrangement common to e-beam controlled laser discharges. The cross-sectional area of the discharge region is typically in the 1-100 cm^2 range and the discharge length in the optical direction is typically on the order of one meter, dimensions corresponding to active volumes in the 0.1 - 10.0 liter range.

efficient excitation of the working species is below that required for self-sustained operation, this method results in a decoupling of the electron production process from the electric field. For this reason a host of plasma instabilities can often be eliminated or their effects greatly reduced (Nighan, 1977a, 1977b). Indeed, this technique has proven successful as a means of producing uniform glow discharges in large volumes ($\gtrsim$ 1 liter) over a continuous range of pressures from a few tenths to several atmospheres, thereby advancing the state of the art in a very substantial way.

A. Application to Electronic Transition Lasers

The basic motivation underlying application of the e-beam controlled discharge technique to electronic transition lasers is the same as that for CO_2 lasers; i.e., creation of scalable, high pressure glow discharges. There the similarity ends, however. Because the CO_2 laser operates on relatively low energy vibrational transitions, the optimum electron temperature is always very much less than that required for self-sustained or regenerative operation. For this same reason, the concentration of electronically excited species remains very low, and multi-step ionization is unimportant. Thus, in CO_2 lasers there are no significant ionization mechanisms other than those provided directly (or indirectly) by the e-beam. By way of contrast, UV and/or visible lasers require efficient excitation of electronic levels very close to the ionization limit; i.e., a high electron temperature is required for efficient excitation. Additionally, large fractional concentrations of easily ionized excited species are invariably present, with

the result that multi-step ionization is usually significant and often dominant. Thus, e-beam controlled electronic transition laser discharges are marginally stable at best, and utilization of this technique for electronic transition laser applications is confined to a relatively limited range of parameter space.

1. Electron Production and Loss

For a spatially uniform, collison dominated plasma medium typical of e-beam sustained electronic transition laser discharges, the electron conservation equation may be expressed in the following illustrative form:

$$\frac{\partial n_e}{\partial t} = nS_{EB} + n_e n k_i(E/n) + n_e n^* k_i^*(E/n) + \ldots - n_e n k_a(E/n) - \ldots \qquad (1)$$

In this equation, in which only the processes usually dominant in rare gas/mercury-halide lasers are indicated, n_e, n^*, and n are the number densities of electrons, electronically excited species (e.g., metastable atoms), and neutrals, respectively; $k_i(E/n)$, $k_i^*(E/n)$, and $k_a(E/n)$ are the <u>mixture weighted</u> rate coefficients for ionization from the ground state, for excited state ionization, and for attachment, respectively; and S_{EB} is the rate of electron production due to the e-beam. Penning ionization, electron-ion recombination, and negative ion detachment, although frequently important, have been omitted for the sake of clarity. As will be shown subsequently, it is often possible to obtain quasi-steady conditions such that the temporal derivative on the left-hand side of Eq. (1) is small compared to the electron production and loss terms. In this circumstance it is

instructional to plot the various contributions to electron production (loss) as a function of E/n. Presented in Fig. 2 is an illustration of the E/n variation of electron production and loss terms under quasi-steady conditions which are typical of e-beam controlled rare gas/mercury-halide laser discharges. This figures indicates that for low values of E/n, ionization resulting from discharge processes* is very small compared to that of the e-beam (Region A). That is, as a consequence of the low electron temperature, ionization from the ground state is insignificant and excited state production is so low that multi-step ionization is not important. In this low E/n regime the rate of electron production due to the e-beam electrons balances the rate of electron loss, the latter process usually dominated by halogen dissociative attachment (Chantry, 1981). Under these circumstances the discharge is truly electron-beam controlled and behaves much like a CO_2 laser discharge under otherwise similar conditions. Unfortunately, in this regime it is not possible to efficiently produce electronically excited species in the required numbers. Efficient excited state production requires that E/n (electron temperature) be increased, and along with such an increase there occurs a rapid increase in both direct ionization of neutrals from their ground states, and multi-step ionization involving the electronically excited species participating in laser molecule formation. Under these circumstances discharge ionization processes become increasingly important, indeed comparable to the ionization produced by the e-beam (Region B). Ultimately, an E/n value is reached above which the ionization process is

* Ionization processes other than the e-beam contribution in Eq. (1).

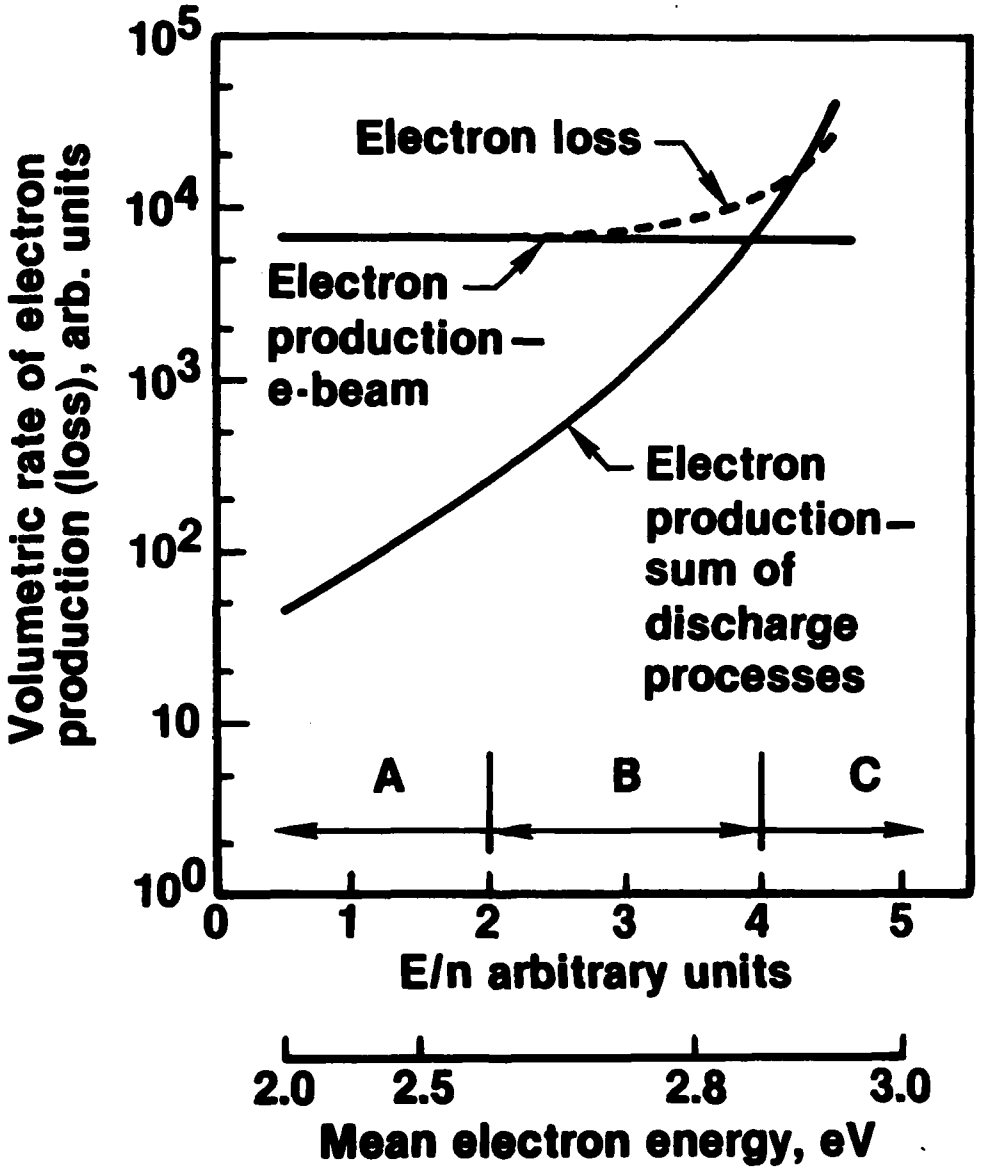

Figure 2. E/n variation of the electron production and loss terms for quasi-steady conditions representative of e-beam controlled rare gas/mercury-halide discharges.

no longer stable, Region C (Nighan, 1978a; Brown and Nighan, 1978; Long, 1979; Haas, 1981; and Rokni and Jacob, 1981). Thus, for e-beam ionized electronic transition laser discharges there exists a relatively narrow E/n "window", bounded at low E/n's by a region of insufficient pumping intensity and at high E/n's by discharge ionization instability. Optimum laser conditions are usually found to exist within the high E/n portion of the stable range, for which ionization by the e-beam may be the largest single source of ionization, but for which the aggregate effect of discharge ionization mechanisms is comparable to or even larger than electron production due to the e-beam alone.

In spite of the constraints discussed above, conditions can usually be found such that the generation of spatially and temporally uniform laser discharges becomes possible. Presented in Fig. 3 are voltage and current profiles representative of an e-beam controlled mercury-bromide laser discharge at a pressure of 2.0 atm. This figure shows that following an initial transient during which the applied discharge voltage rises, there results a highly uniform discharge having a duration of almost 1 μsec, as evidenced by the essentially constant values of voltage and current. Since characteristic collison times are typically less than Q.1 μsec for such conditions, analysis shows that kinetic processes in the plasma medium are essentially quasi-steady throughout the discharge pulse, as suggested by the trend exhibited by the V-I characteristics shown in the figure. Analysis of such a medium has proven invaluable as a tool to identify the mechanisms

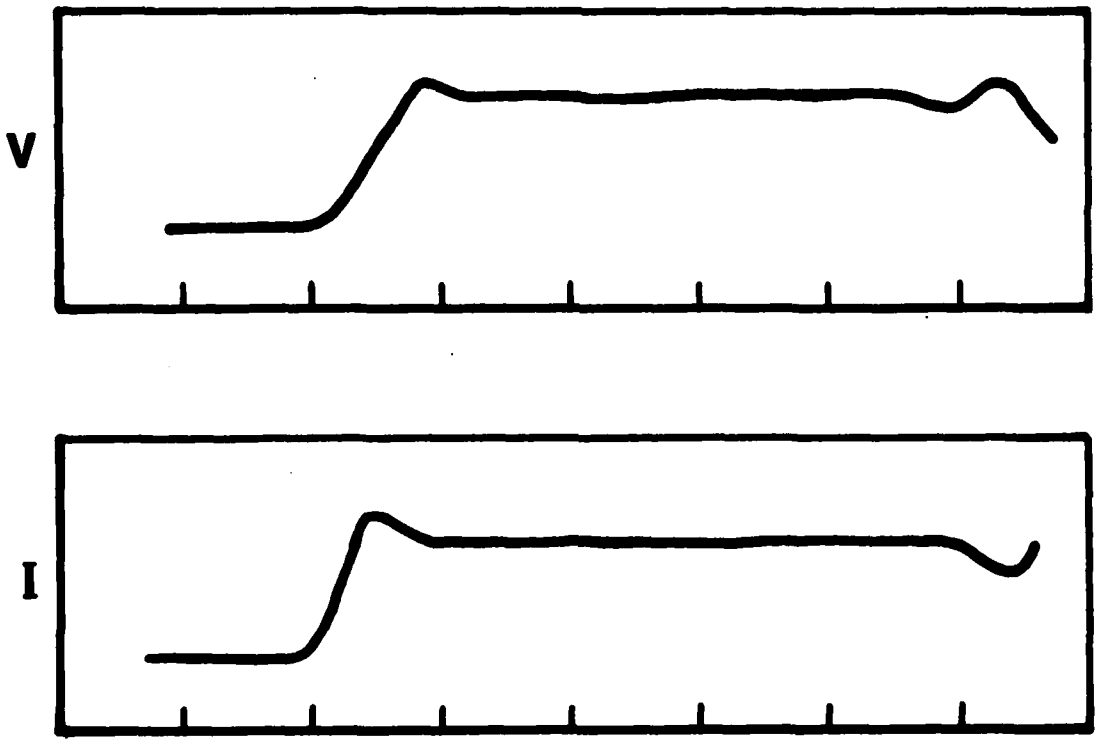

Figure 3. Representative current-voltage characteristics for an e-beam controlled mercury-bromide laser discharge..

controlling both discharge and laser operation (Nighan, 1978a; Rokni, et al., 1978).

III. RARE GAS-HALIDE AND MERCURY-HALIDE LASERS

Because of their high efficiency (1-10%) and scalability, electrically excited rare gas and mercury-halide lasers have been the subject of intensive investigation in recent years. The characteristics and performance features of these lasers are treated in detail in the contributions to this volume by Rokni and Jacob (1981) and Parks (1981). Of the several members comprising this class of lasers, the XeCl (308 nm) laser using HCl as a halogen donor, and the HgBr (502 nm) laser utilizing dissociative excitation of the mercuric-bromide molecule ($HgBr_2$) have unusual promise for many applications. The primary reasons for the success of these lasers are favorable absorption characteristics permitting high optical extraction efficiency, combined with relatively minor volumetric and/or surface chemistry problems. These attributes are due in large measure to the use of HCl (Champagne, 1978) and $HgBr_2$ (Schimitschek et. al., 1977 and Schimitschek and Celto, 1978) as the respective halogen donors in XeCl and HgBr lasers. Indeed, the XeCl laser has demonstrated lifetime characteristics setting it apart from others of this general class (McKee, et al, 1980; Gower, et al, 1980; and Miller et al, 1979).

In this section the basic kinetic sequences operative in e-beam ionized XeCl($B \rightarrow X$) and HgBr($B \rightarrow X$) laser discharges will be briefly outlined,

emphasizing certain unique features characteristic of HCl and $HgBr_2$. Specifics of the XeCl and HgBr laser media will be discussed in Section IV.

A. XeCl(B → X) Laser Discharges

Although one of the first rare gas-halide lasers to exhibit oscillation, efficient XeCl laser operation was not achieved until HCl was used as the halogen donor. The reduction in absorption at the laser wavelength accompanying use of HCl in Xe-Ne mixtures resulted in the achievement of electrical-optical energy conversion efficiency in the 6.0-7.0% range using pure electron-beam excitation (Champagne, 1978), and in the 2.0-3.0% range using the e-beam ionized discharge method of primary interest here (Nighan and Brown, 1980).

The sequence diagram of Fig. 4 illustrates the dominant features of the XeCl formation chain in discharge excited lasers. Under optimum conditions, calculations show that electron energy transfer is dominated by Xe metastable atom production and by subsequent excitation of metastable atoms to the higher lying manifold of Xe 6p states (Nighan and Brown, 1980). Production of the ion Xe^+ then proceeds by way of electron impact ionization of both Xe metastable (6s) and p-state atoms. As indicated in the figure, the Cl^- negative ion is produced by dissociative attachment to vibrationally excited HCl, and subsequently recombines with Xe^+ in a three-body reaction resulting in formation of the laser molecule XeCl(B). Thus, XeCl(B) is produced by way of an ion-recombination channel with an efficiency in the 5-20% range depending on specific conditions.

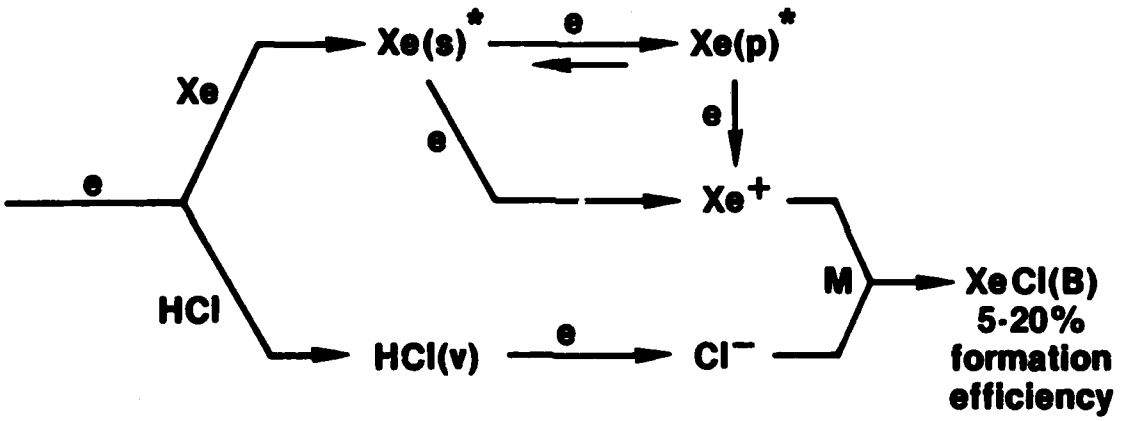

Figure 4. Sequence diagram showing the dominant processes in the XeCl(B) formation chain in discharge excited Ne-Xe-HCl mixtures (from Nighan and Brown, 1980).

1. Vibrational Excitation and Dissociative Attachment of HCl

There are several important features, only recently understood, which set HCl apart from the halogen donors used in other rare gas-halide lasers. Unlike most chlorine donors, formation of XeCl(B) by way of $Xe(^3P_2)$-HCl reactions is slightly endothermic at 300°K, reflecting the large 4.45 eV HCl bond energy. Although $Xe(^3P_1, ^3P_0, ^1P_1)$-HCl reactions or $Xe(^3P_2)$-HCl($v \gtrsim 1$) reactions are energetically capable of XeCl(B) formation, available evidence indicates that such reactions are dominated almost entirely by the dissociation of HCl rather than by XeCl(B) formation (Kolts, et al, 1979; Wren and Setser, 1981; and Tang, et al, 1981). Thus, it can be concluded with reasonable certainty that Xe^* quenching by HCl is not a significant XeCl(B) formation process in discharge excited lasers. Additionally, initial evaluation of the role of HCl attachment indicated that formation of Cl^- at a rate sufficient for XeCl(B) formation by way of the Xe^+-Cl^- recombination channel was not possible. This conclusion was based largely on the relatively small Cl^-/HCl cross section measured by Azria, et al (1974), and by others as well. However, HCl has an unusually large cross section for vibrational excitation (Rohr and Linder, 1976), a circumstance resulting in a very large fractional concentration of vibrationally excited HCl under XeCl laser conditions. By considering this factor in an analysis of experimental data obtained using a variety of HCl containing mixtures excited in e-beam controlled discharges, Nighan and Brown (1980) concluded that vibrational excitation of HCl resulted in more than an order-or-magnitude increase in

Cl^- production over that to be expected from HCl in its ground vibrational state. This finding was subsequently confirmed by measurements of the threshold values of the cross sections for $Cl^-/HCl(v = 1, 2)$, (Allan and Wong, 1981). Thus, vibrational excitation of HCl has been found to be a fundamental process in XeCl lasers, acting as a precursor to production of Cl^- by way of dissociative attachment.

Presented in Fig. 5 are the rate coefficients for excitation of HCl from the ground state to the first vibrational level, and for the Cl^-/HCl ($v = 0$) dissociative attachment reaction, as computed for a Ne-Xe-HCl laser mixture. The measurements of Rohr and Linder (1976) indicate that the $v = 0 \rightarrow 2$ and $v = 0 \rightarrow 3$ transitions in HCl have cross sections very much smaller than the $v = 0 \rightarrow 1$ transition. Thus, multi-quantum vibrational transitions are unlikely to be important, and the rate coefficient for the $v = 0 \rightarrow 1$ transition shown in Fig. 5 is probably representative of single quantum transitions involving higher HCl vibrational levels as well. On this basis Nighan and Brown (1980) have modeled XeCl e-beam controlled laser discharges and, based on analysis of laser/discharge characteristics, have inferred an <u>effective</u>* rate coefficient for the reaction $Cl^-/HCl(v)$, the magnitude of which is indicated by the shaded region of Fig. 5. Although the energy variation of the attachment cross sections for HCl vibrational levels are not yet known, Allan and Wong (1981) have observed an exceptionally

---

* The effective attachment coefficient used here refers to the average over all HCl vibrational levels; i.e., $k_a(\text{eff}) \equiv [HCl]^{-1} \Sigma HCl(v) k_a(v)$.

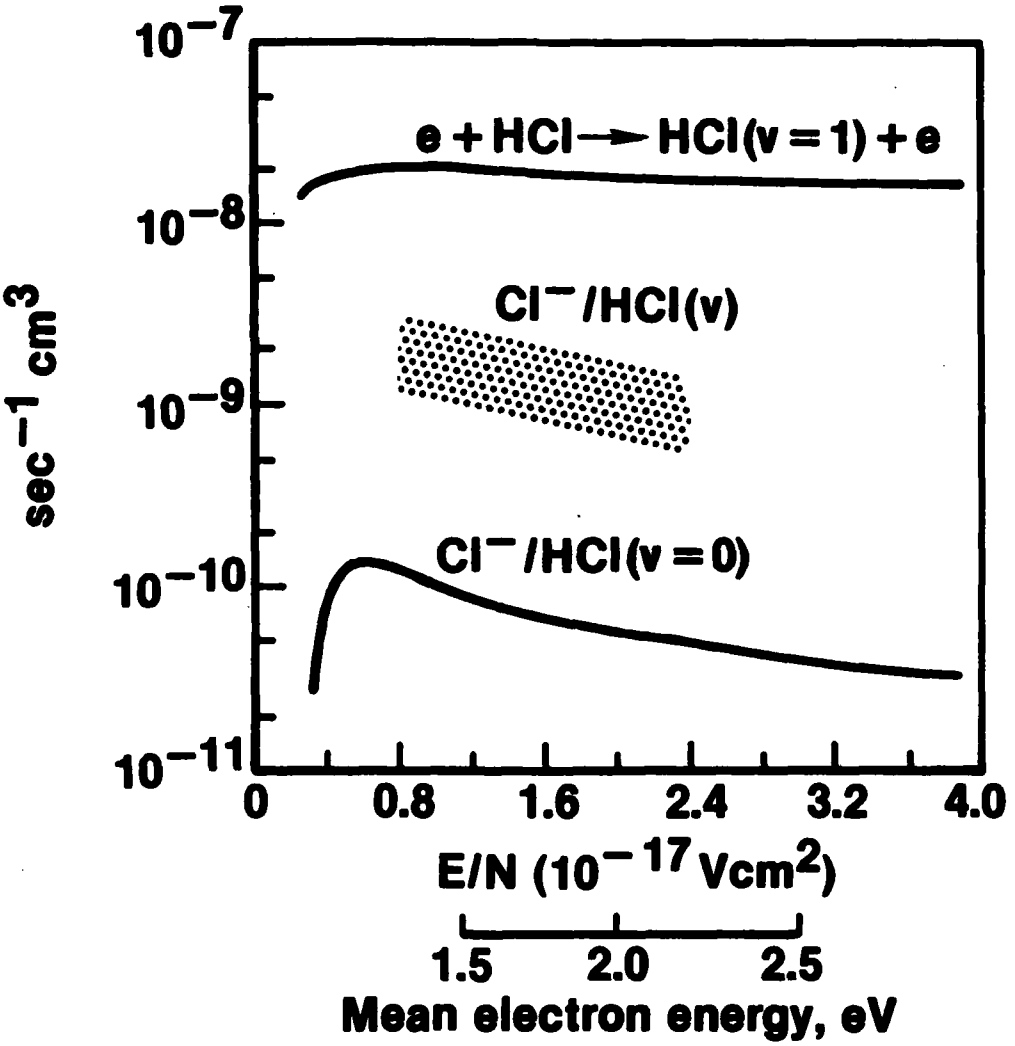

Figure 5. Rate Coefficients for vibrational excitation and dissociative attachment for HCl in the ground vibrational state, computed for a Ne(0.989)-Xe(0.01)-HCl(0.001) laser mixture. The shaded region is indicative of the magnitude of the effective rate coefficient for attachment to vibrationally excited HCl (from Nighan and Brown, 1980).

strong dependence of the Cl^-/HCl attachment process on temperature, and have inferred $\sigma(v = 1)/\sigma(v = 0)$ and $\sigma(v = 2)/\sigma(v = 0)$ ratios of approximately 38 and 880, respectively, at the energies corresponding to the thresholds for each attachment process. Numerical experimentation has shown that this finding is quantitatively consistent with the interpretation of Nighan and Brown (1980). Thus, there is ample evidence that HCl is unique among the rare gas-halide laser halogen donors, exhibiting relatively weak attachment until vibrationally excited, a characteristic impacting significantly on both discharge and laser properties.

B. $HgBr(B)/HgBr_2$ Dissociation Laser Discharges

The closely related mercury-halide lasers $HgBr(B \rightarrow X)$ and $HgCl(B \rightarrow X)$ exhibited relatively efficient laser oscillation shortly after rare gas-halide oscillation was demonstrated (Parks, 1977a, 1977b). Initially the HgBr laser was excited using mixtures containing mercury and various bromine compounds. However, practical problems encountered at the high temperatures needed to produce the required concentration of Hg are formidable. Additionally, the reaction sequence typical of such mixtures is non-cyclic resulting in significant temporal changes in mixture composition. These factors signficantly retarded progress in $HgBr(B \rightarrow X)$ laser development. However, Schimitschek and Celto (1978, 1980) demonstrated that dissociative excitation of the mercuric bromide molecule ($HgBr_2$) resulted in relatively efficient HgBr(B) formation. Moreover, the required concentrations of $HgBr_2$ can be obtained at temperatures less than 200°C. Additionally, repetitive

pulsing and related discharge lifetime tests demonstrated that volumetric and surface chemistry problems associated with the use of $HgBr_2$ are relatively minor compared to those encountered using mixtures containing mercury and bromine compounds, and that the $HgBr(B)/HgBr_2$ reaction sequence is cyclical. For these reasons use of a molecular species comprising the mercury-halide molecule itself represented a significant step toward development of a practical visible wavelength laser.

1. $HgBr_2$ Dissociative Excitation

Efficient $HgBr(B \rightarrow X)$ laser oscillation has been achieved in discharge excited mixtures containing N_2 and $HgBr_2$ (Schimitschek and Celto, 1980), and in $Xe-HgBr_2$ mixtures (Brown and Nighan, 1980). Analysis of discharge and laser properties has shown that HgBr(B) is produced in these lasers as a consequence of dissociative excitation of $HgBr_2$, following quenching by ground state $HgBr_2$ molecules of either $N_2(A^3\Sigma_u^+)$, and probably higher energy N_2^* states, or $Xe(^3P_2)$ (Nighan, 1980; Brown and Nighan, 1980). The dominant steps in the HgBr(B) excitation sequence are indicated in the simplified energy level diagram presented in Fig. 6. In N_2-HgBr_2 mixtures $N_2(A^3\Sigma_u^+)$ and a host of higher lying N_2 electronic states are produced by electron impact excitation of ground state N_2. Excitation transfer to the predissociating $^3\Sigma_u^+$ (or $^1\Sigma_u^+$) state of $HgBr_2$ results in HgBr(B) formation as indicated in the figure (Wadt, 1980). Although an intrinsic laser efficiency of about 1% is obtained routinely using mixtures containing N_2, relatively inefficient utilization of the energy transferred to N_2 states higher than the $A^3\Sigma_u^+$ state,

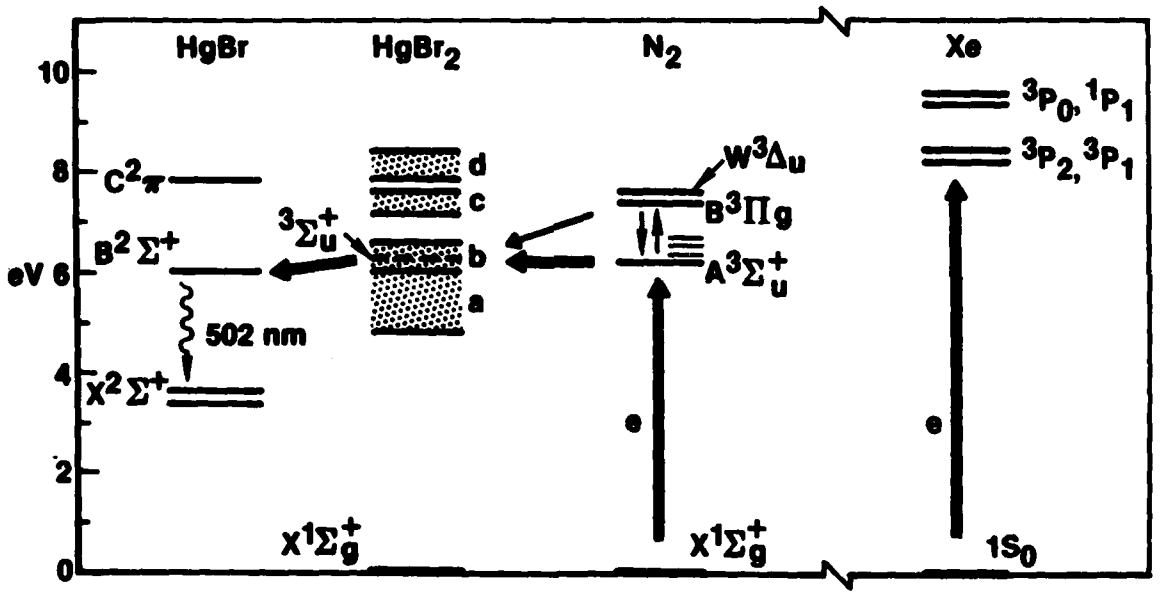

Figure 6. Simplified energy level diagram illustrating the dominant steps in the HgBr(B) formation sequence in $HgBr_2$ dissociation laser discharges using either N_2 or Xe as the energy receptor-transfer species.

along with energy loss due to N_2 vibrational excitation, may limit HgBr laser efficiency to the 1.0 - 2.0% range when N_2 is used as the energy transfer species (Nighan, 1980). By way of contrast, the Xe($^3P_2$) metastable atom has a very large rate for $HgBr_2$ dissociative excitation, resulting in HgBr(B) formation with near unit efficiency (Chang and Burnham, 1980). In addition, calculations show that electronic excitation of Xe($^3P_2$) is substantially more selective (i.e., efficient) than is N_2 electronic excitation. Indeed, initial use of Xe in place of N_2 has resulted in HgBr(B → X) laser efficiency in the 2.0 - 3.0% range, suggesting that even higher efficiency may be possible (Brown and Nighan, 1980). In either case, however, HgBr(B) is produced by way of an excitation transfer channel in contast to the ion recombination reaction dominant in XeCl lasers.

2. Ionization and Dissociative Attachment of $HgBr_2$

Although both N_2 and Xe are used as energy receptor-transfer species in HgBr(B)/$HgBr_2$ dissociation lasers, most characteristics of the resulting laser discharges are far different than would be expected on the basis of the known differences between N_2 and Xe electron energy transfer processes alone. However, the observed differences are understood and provide a particularly interesting illustration of the importance to laser analysis of accurate and complete cross section data.

Figure 7 presents computed electron energy distribution functions in two Ne-$HgBr_2$ mixtures, each containing either 10% N_2 or Xe. It requires a

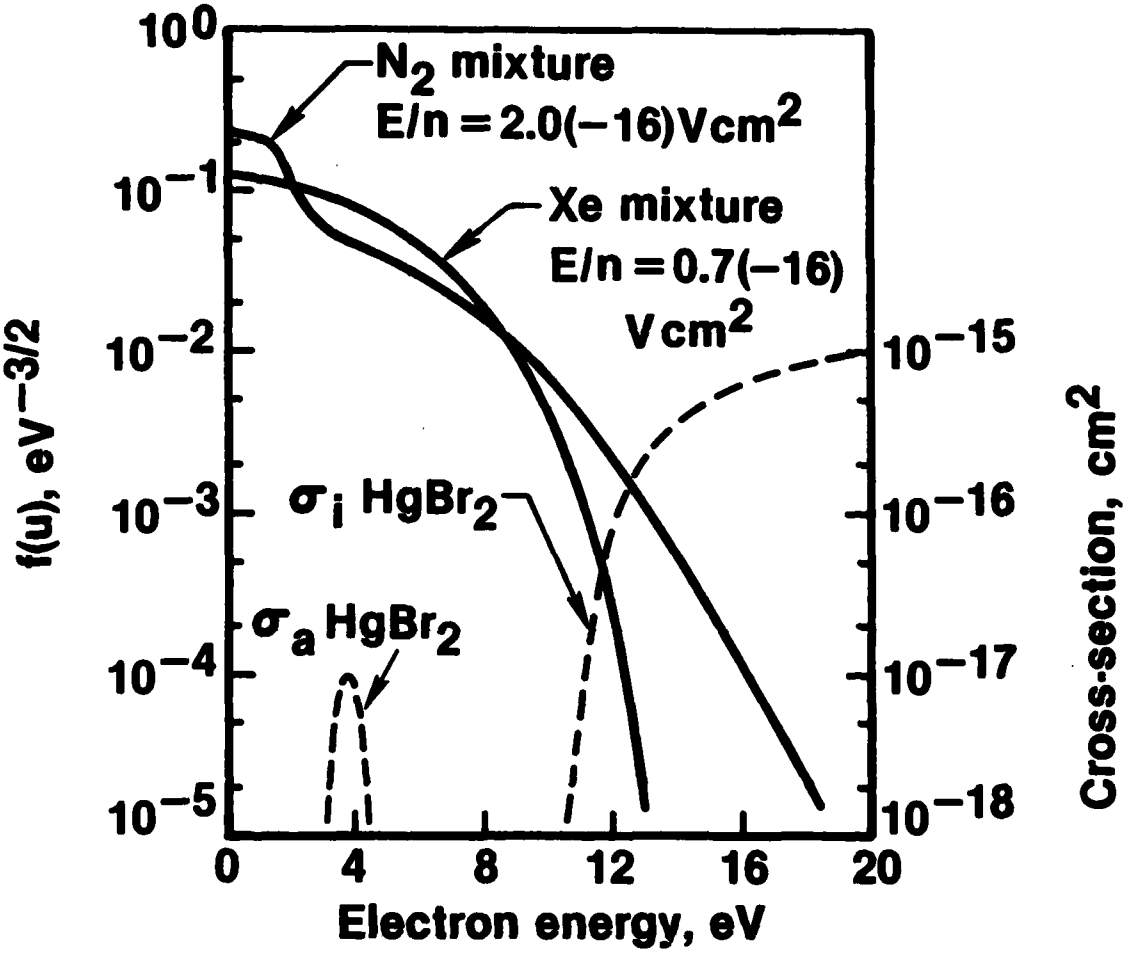

Figure 7. Computed electron-energy distributions in Ne-$HgBr_2$ mixtures containing either 10% N_2 or 10% Xe. Also shown are the cross sections for $HgBr_2$ dissociative attachment and ionization (from Wiegand and Boedeker, 1981).

significantly larger E/n value to produce the same mean electron energy* in the N_2 mixture, reflecting the large energy loss due to N_2 vibrational excitation. Thus, for the purpose of this illustration, E/n has been chosen for both the Xe and N_2 mixtures to yield approximately the same mean electron energy. Figure 7 illustrates the familiar, albeit unusual, shape of the electron energy distribution in N_2 (Nighan, 1970). In N_2 the energy distribution is significantly depleted in the 2-5 eV range within which the N_2 vibrational cross sections are very large (Schulz, 1976). However, in the Xe mixture there is an excess of electrons in the 2-5 eV range, but a severe depletion above the 8.3 eV Xe($^3P_2$) excitation threshold. These characteristics of electron energy transfer collisions with N_2 and Xe, respectively, have a dramatic effect on the electron energy distribution as E/n is varied, and on the effectiveness of $HgBr_2$ as an attaching species under laser conditions.

Figure 7 also shows the cross sections for $HgBr_2$ dissociative attachment and ionization (Wiegand and Boedeker, 1981). The $HgBr_2$ attachment cross section has a relatively narrow energy width, and happens to reach its peak value at an energy about 2.0 eV higher than the onset of the resonant portion of the N_2 vibrational cross sections; i.e., in the region of electron depletion in the N_2 laser mixture. Additionally, $HgBr_2$ has a relatively low ionization potential (10.62 eV) and a very large ionization cross section in the region of depleted electrons in the Xe laser mixture. Thus, as E/n is

---

* Mean electron energy as used is defined as 2/3 the average electron energy; i.e., kT_e/e for a Maxwellian energy distribution.

varied, calculations show that ionization of $HgBr_2$ is weighted much less heavily in the Xe mixture than in the N_2 mixture, and attachment is weighted much less heavily in the N_2 mixture than in the Xe mixture. The signficance of this situation is vividly illustrated by comparing attachment coefficients and the net or apparent effect of attachment for Ne-$HgBr_2$ mixtures containing the same amount of N_2 and Xe, respectively.

Presented in Fig. 8 are the results of such a calculation over the complete range of E/n appropriate for laser excitation of these mixtures. Figure 8 shows that the attachment coefficient in the Xe mixture is almost completely insensitive to E/n, reflecting the relatively small changes in the electron energy distribution in the 3-5 eV range as E/n is varied. However, since the $HgBr_2$ ionization cross section is very large, the net effect of $HgBr_2$ as a species contributing to electron loss in the Xe mixture diminishes rapidly as E/n is increased, as is evidenced by the decrease in the difference between the attachment and ionization coefficients, $k_a - k_i$. Indeed, for E/n greater than about 1.4×10^{-16} Vcm^2 in the Xe mixture, $HgBr_2$ ionization dominates over attachment; that is, $HgBr_2$ makes a net contribution to electron production rather than loss. The behavior of the N_2 mixture is markedly different qualitatively and quantitatively. For low E/n values in N_2 dominated mixtures, the electron distribution function is truncated at about 2.0 eV, the onset of the resonant portion of the N_2 vibrational cross sections (Schulz, 1976). Eventually electrons penetrate the vibrational barrier at higher E/n values. However, the nature of the electron distribution

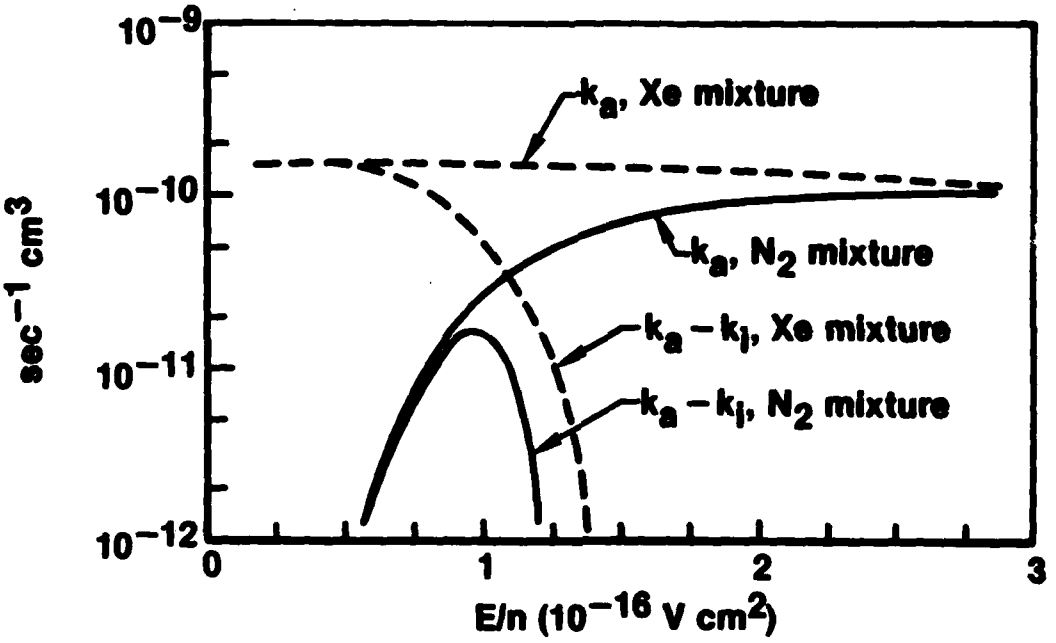

Figure 8. Computed $HgBr_2$ attachment coefficients in Ne-$HgBr_2$ mixtures containing either 10% N_2 or 10% Xe. Also shown is the net or effective attachment coefficient for each mixture, as defined by the difference between the $HgBr_2$ attachment and ionization coefficients, k_a-k_i.

function results in a strong E/n dependence of the $HgBr_2$ attachment coefficient. More importantly, when the $HgBr_2$ ionization coefficient in the N_2 mixture is subtracted from the attachment coefficient, Fig. 8 shows that the net or apparent attachment coefficient has a very unusual behavior, and is much smaller than the corresponding value in Xe over the entire E/n range. Indeed, with a maximum $k_a - k_i$ value only slightly above 1.0 x 10^{-11} $sec^{-1}cm^3$ in the N_2 mixture (one-tenth of the maximum value in the Xe mixture), $HgBr_2$ does not behave like an attaching species for the conditions typical of laser discharges. Calculations show that for the same ion densities and $HgBr_2$ concentrations, attachment is the dominant electron loss process in the Ne-Xe-$HgBr_2$ laser mixture, and recombination and dominant electron loss in the corresponding Ne-N_2-$HgBr_2$ mixture. Clearly, interpretation of the resulting discharge/laser characteristics without benefit of the HgBr ionization and attachment cross sections would be a difficult task indeed.

IV. EXCITED STATE AND IONIC KINETICS

Recognition of the potential of rare gas-halides as UV laser molecules, and the following very rapid development of electrically excited lasers provided great stimulus for research in a number of important areas, particularly, energy transfer reactions involving the rare gas metastable states and halogenated molecules (Velazco, et al, 1978), electron-halogen dissociative attachment (Chantry, 1981), and high pressure ion-ion recombination

reactions (Flannery, 1979, 1981). As a consequence, understanding of such processes has reached a new plateau, and a wealth of fundamental data have been generated, thereby providing the basis for development of sophisticated analytical models of laser/discharge characteristics (Rokni, et al, 1978; and Nighan, 1978a). A very significant feature of such models is their ability to generate information relating to fundamental processes not easily accessed experimentally. For this reason, interpretation of experimental results using analytical models has itself resulted in identification of many previously unrecognized processes, and has contributed to the generation of additional basic data as well (Nighan, 1978b; Nighan and Brown, 1980; and Morgan and Szoke, 1981). As an illustration of the information typically obtained using the now well-developed kinetic modeling techniques, in this section results representative of e-beam ionized XeCl and HgBr laser discharges will be presented.

A. Ionic and Excited State Processes In XeCl(B → X) Laser Discharges

1. General Characteristics

As mentioned in Section I, rare gas-halide lasers are excited electrically using a variety of techniques. Although the resulting laser media share some common characteristics, specific differences in the excitation methods introduce substantial changes in important processes, including the rare gas-halide formation sequence itself. Nighan and Brown (1980) have modeled the characteristics of e-beam ionized XeCl laser discharges for conditions of relatively high gain and XeCl(B) formation efficiency, as

verified by experimental observations. For conditions typical of this excitation technique, optimum laser characteristics are obtained using neon as a buffer gas at a total pressure of 3.0 - 5.0 atm, containing 1-2% Xe and approximately 0.1% HCl. In such a mixture the neon provides the stopping agent for the ionizing high energy beam electrons (Jacob, 1981), and also serves to ensure effective vibrational relaxation of the XeCl(B) vibrational manifold. Additionally, volumetric absorption at the laser wavelength due to excited and ionic states of neon is minimal (Champagne, 1981). Although Xe is the working species, its concentration is limited to a very low level so as to prevent excessive formation of Xe_2^+ which is a strong absorber at the 308 nm laser wavelength (Champagne, 1981; Michels, et al, 1979a, 1979b). The optimum concentration of HCl results as a compromise between the formation of Cl^- required for XeCl(B) production, and HCl quenching of XeCl(B) and Xe^*, the latter species a precursor of Xe^+ (Fig. 4).

The fact that XeCl(B) is formed by way of an ion-ion recombination reaction, combined with the constraints on the mixture fractions discussed above, results in a low impedance discharge medium having a high current density and low E/n value. Nighan and Brown (1980) have shown that such e-beam ionized XeCl laser discharges actually operate in a quasi-avalanche mode, with only about 10% of the ionization provided by the e-beam, the dominant ionization process being multi-step ionization of Xe excited states by low energy discharge electrons (Fig. 4). For this reason, the term electron-beam <u>assisted</u> discharge has been used to describe this XeCl laser excitation

TABLE I: Representative medium properties for the electron-beam assisted XeCl laser discharge conditions of Nighan and Brown (1980)[a]

Mixture	Pressure	e-beam current density	Discharge current density	E/n	Electric power density	XeCl(B) formation efficiency	Zero-field gain coefficient	Volumetric absorption coefficient
Ne: 0.989 Xe: 0.01 HCl: 0.001	3 atm	$1.5 A cm^{-2}$	$189 A cm^{-2}$	$1.95 \times 10^{-17} V cm^2$	$288 kW cm^{-3}$	17.2%	$6.7\% cm^{-1}$	$0.67\% cm^{-1}$

a. The tabulated properties correspond to nearly quasi-steady conditions at a time 0.25 μsec into a 0.5 μsec discharge pulse, at the end of which the time integrated XeCl(B) and electrical energy densities were 7.5 joules/liter and 60 joules/liter, respectively, and for which approximately 95% of both the ionization and energy deposition were provided by the discharge.

procedure (Nighan and Brown, 1980). Other characteristics of this laser discharge are summarized in Table I.

2. Species Concentrations

Presented in Figs. 9 and 10 are computed concentrations of ionic and excited species corresponding to the conditions of Table I. Reflecting the relatively large current density-low E/n conditions, Fig. 9 shows that the electron density is approximately 1×10^{15} cm^{-3}, a relatively high value for a large volume glow discharge of the type under consideration. Indeed, electron quenching of the XeCl(B) laser molecule is comparable to the radiation loss for electron density values above approximately 3×10^{14} cm^{-3} (Rokni and Jacob, 1981). The ion Xe^+, produced by multi-step ionization, is the dominant positive ion in spite of the fact that the total pressure is 3.0 atm. This is a result of (and the reason for) the low fractional concentration of Xe which limits the rate of Xe_2^+ dimer ion formation. Nonetheless, even though the Xe_2^+ concentration is more than an order of magnitude less than that of Xe^+, volumetric absorption at the laser wavelength due to Xe_2^+ photodissociation represents about one-third of the total absorption for these conditions. Thus, increasing the Xe fractional concentration to a value much above 1% results in a nearly proportional increase in volumetric absorption, along with a decrease in optical extraction efficiency (McCusker, 1979).

Although Cl^- is produced at a rapid rate by dissociative attachment to vibrationally excited HCl, the relatively low HCl concentration combined

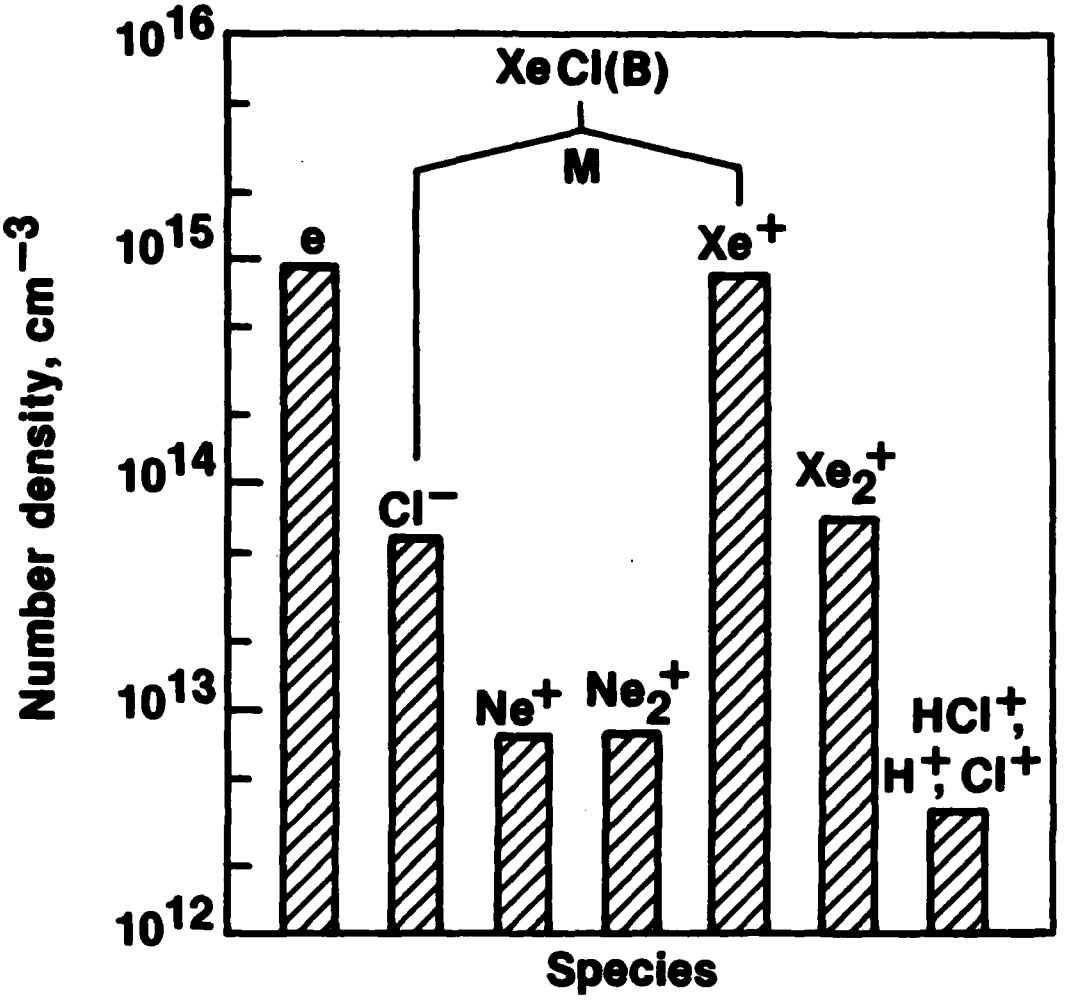

Figure 9. Computed quasi-steady charged particle concentrations for the e-beam assisted XeCl laser discharge conditions of Table I.

with a very large Cl^- loss rate due to the Cl^--Xe^+ XeCl(B) formation process results in a Cl^- concentration which is low compared to the electron and Xe^+ densities. Even so, absorption at the laser wavelength due to electron photodetachment of Cl^- (Rothe, 1969) contributes about 15% to the total volumetric absorption for these conditions.

Figure 10 shows that the corresponding concentrations of Xe^* (representing the coupled $^3P_2$ and $^3P_1$ 6s states) and the grouped levels of the 6p manifold are very high and of comparable magnitude. Ionization from these states dominates Xe^+ formation as discussed previously. The high $Xe^*(p)$ concentration impacts on laser/discharge properties in several ways: photoionization at the laser wavelength by p state atoms (Hyman, 1977, Duzy and Hyman, 1980), a disproportionate contribution by p states to multi-step ionization (Hyman, 1979; and Nighan, 1978a), and energy loss by way of p-s relaxation by neutral collisions (Nighan, 1978a; and Sec. IV-D herein). The concentration of laser molecules, $XeCl^*(B)$, is shown to exceed 10^{14} cm^{-3} corresponding to a gain of over 5% cm^{-1}; calculations also indicate that the XeCl(B) formation efficiency is in the 15-20% range for these conditions (Table I). In addition, Fig. 10 shows that the concentration of the triatomic rare gas-halide molecule, Xe_2Cl^*, is almost as large as that of $XeCl^*(B)$. The molecule Xe_2Cl^* is formed as a result of a three-body $XeCl^*(B)$ quenching reaction involving Xe (Tang, et al, 1981), and for these conditions is produced with an energy efficiency of approximately 1%. Although Xe_2Cl^* formation is a loss process in the XeCl(B → X) laser, electrical excitation of similar

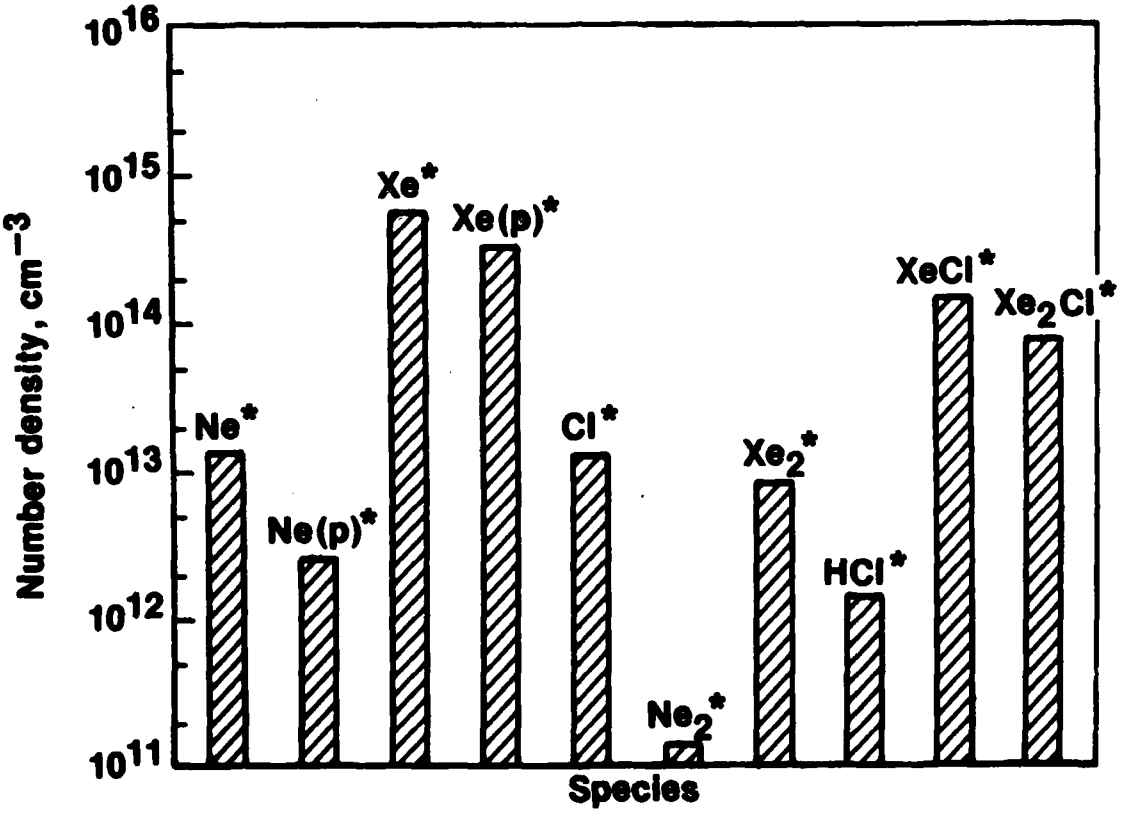

Figure 10. Computed quasi-steady excited state concentrations for the e-beam assisted XeCl laser discharge conditions of Table I.

mixtures containing 5-10% Xe have resulted in Xe_2Cl^* laser emission centered at 518 nm (Tittel, et al, 1980).

B. Ionic and Excited State Processes in the HgBr(B)/$HgBr_2$ Dissociation Laser Discharge

1. General Characteristics

The blue/green HgBr(B → X)/$HgBr_2$ dissociation laser operating at 502 nm is in a somewhat earlier stage of development than its UV XeCl(B → X) counterpart. This laser, first excited electrically using a fast-pulse, avalanche discharge technique (Schimitschek and Celto, 1978, 1980), and more recently using the e-beam controlled discharge method (Brown and Nighan, 1980), operates with a neon buffer at a pressure of 1.5 - 3.0 atm at a temperature in the 150 - 200°C range. Neon is used as the buffer for many of the same reasons discussed in connection with the XeCl laser. Variation of the temperature between 150 - 200°C range results in an $HgBr_2$ vapor pressure variation in the range 2.0 - 20.0 torr (Brewer, 1950). Both N_2 or Xe at fractional concentrations of 5-10% have been used successfully as the discharge energy receptor-transfer species (Schimitschek and Celto, 1980; and Brown and Nighan, 1980). As discussed previously, the principal factors determining the mixture constituents and their respective fractions in rare gas-halide lasers, such as XeCl, are absorption at the laser wavelength and collisional quenching of the laser molecule. However, the HgBr(B) molecule is apparently much less susceptible to collisional deactivation than the rare gas-halides (Roxlo and Mandl, 1980); and therefore mixture optimization in the $HgBr_2$ dissociation laser appears to be somewhat less critical than is

the case in the XeCl laser, for example. However, very little information exists concerning absorption by ionic and excited species in the visible region of the spectrum. For this reason it is likely that as cross sections for absorption at wavelengths in the blue/green region become available, the choice of mixture fractions and even the specific constituents of the HgBr(B)/$HgBr_2$ laser will be affected. In order to facilitate comparisons with the XeCl laser conditions, treated previously, the discussion to follow will focus attention on conditions typical of the HgBr(B)/$HgBr_2$ dissociation laser using Xe as the energy transfer species.

2. Species Concentrations

The fact that the HgBr(B) molecule is produced by way of an excitation transfer reaction relieves the requirement for high ion density typical of ion recombination lasers such as XeCl. Efficient production of the excitation transfer species (e.g., $Xe(^3P_2)$) is possible for conditions such that an electron-beam ionized discharge operates in a high impedance mode corresponding to a low current density and high E/n value, a situation also typical of the KrF^* laser discharge (Nighan, 1978a). For these circumstances the discharge ionization process is dominated by the e-beam (Brown and Nighan, 1980), although discharge ionization processes remain significant ($\sim$ 25-40% of the total) for the reasons discussed in Section II. Typical characteristics of such a laser discharge using Xe as the energy transfer species are summarized in Table II.

TABLE II: Representative medium properties for the electron-beam controlled HgBr laser discharge conditions of Brown and Nighan (1980)[a]

Mixture	Temperature and Pressure	e-beam current density	Discharge current density	E/n	Electric power density	HgBr(B) formation efficiency	Zero-field gain coefficient	Volumetric absorption coefficient
Ne: 0.893 Xe: 0.10 $HgBr_2$: 0.007	185°C 2atm	$0.5 Acm^{-2}$	$13.5 Acm^{-2}$	$7.5 \times 10^{-17} Vcm^2$	$33\ kWcm^{-3}$	19.3%	4.3% cm^{-1}	--

a. The tabulated properties correspond to nearly steady-state conditions at a time 0.5 μsec into a 1.0 μsec discharge pulse, at the end of which the time integrated HgBr(B) and electrical energy densities were 6.7 joules/liter and 35 joules/liter, respectively, and for which the discharge accounted for approximately 90% of the energy deposited and 30% of the ionization.

Figure 11 presents computed ion concentrations for the conditions of Table II. The most obvious manifestation of the high impedance mode of operation is an electron density much less than that of the XeCl laser (Fig. 9). Additionally, the dominant ion is a molecular species, $HgBr_2^+$, which is produced primarily by direct electron impact on ground state $HgBr_2$, and to a lesser extent by charge transfer reactions (Johnsen and Biondi, 1980). Although the laser molecule HgBr(B) can be produced by either electron or Br^- ion recombination with $HgBr_2^+$, calculations show that such reactions are not important for the conditions of Fig. 11. Additionally, recombination reactions are not selective, resulting in many $HgBr_2$ states which do not predissociate with HgBr(B) as a product (Wadt, 1980). Thus, ion reactions in the HgBr(B)/$HgBr_2$ laser are much less important than is the case in the XeCl laser*. However, should $HgBr_2^+$ have an absorption cross section greater than 1×10^{-17} cm^2 near 500 nm, a large concentration of this ion as indicated in Fig. 11 would contribute significantly to volumetric absorption of the medium; thereby limiting optical extraction efficiency.

The corresponding excited state concentrations presented in Fig. 12 are more nearly comparable in magnitude to those in the XeCl laser (Fig. 10). For these conditions $Xe^*(6s)$ is produced very efficiently, subsequently transferring its energy to $HgBr_2(^3\Sigma_u^+)$ which predissociates to form HgBr(B).

* In HgBr(B → X) laser mixtures containing only $HgBr_2$ and neon as a buffer, calculations show that $HgBr_2^+$ recombination with electrons and B_r^- are the processes most likely resulting in HgBr(B) formation.

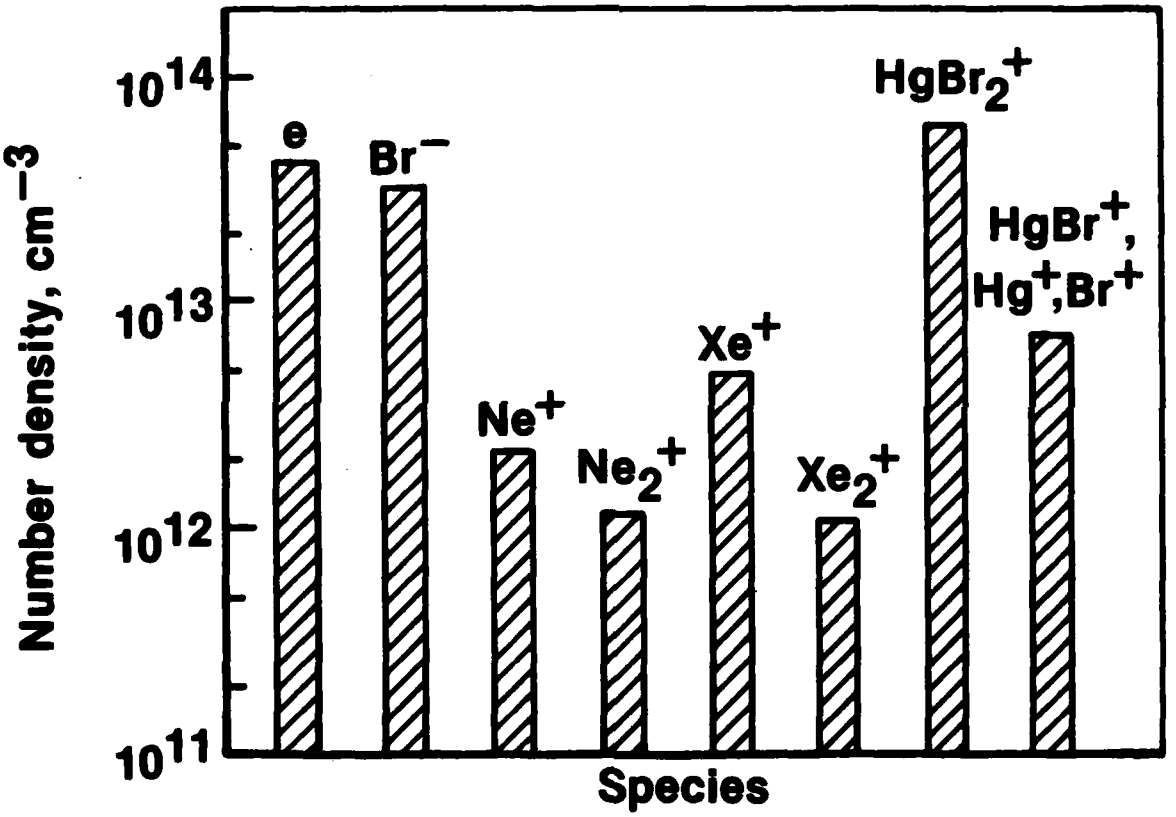

Figure 11. Computed quasi-steady charged particle concentrations for the e-beam controlled HgBr(B)/$HgBr_2$ dissociation laser discharge conditions of Table II.

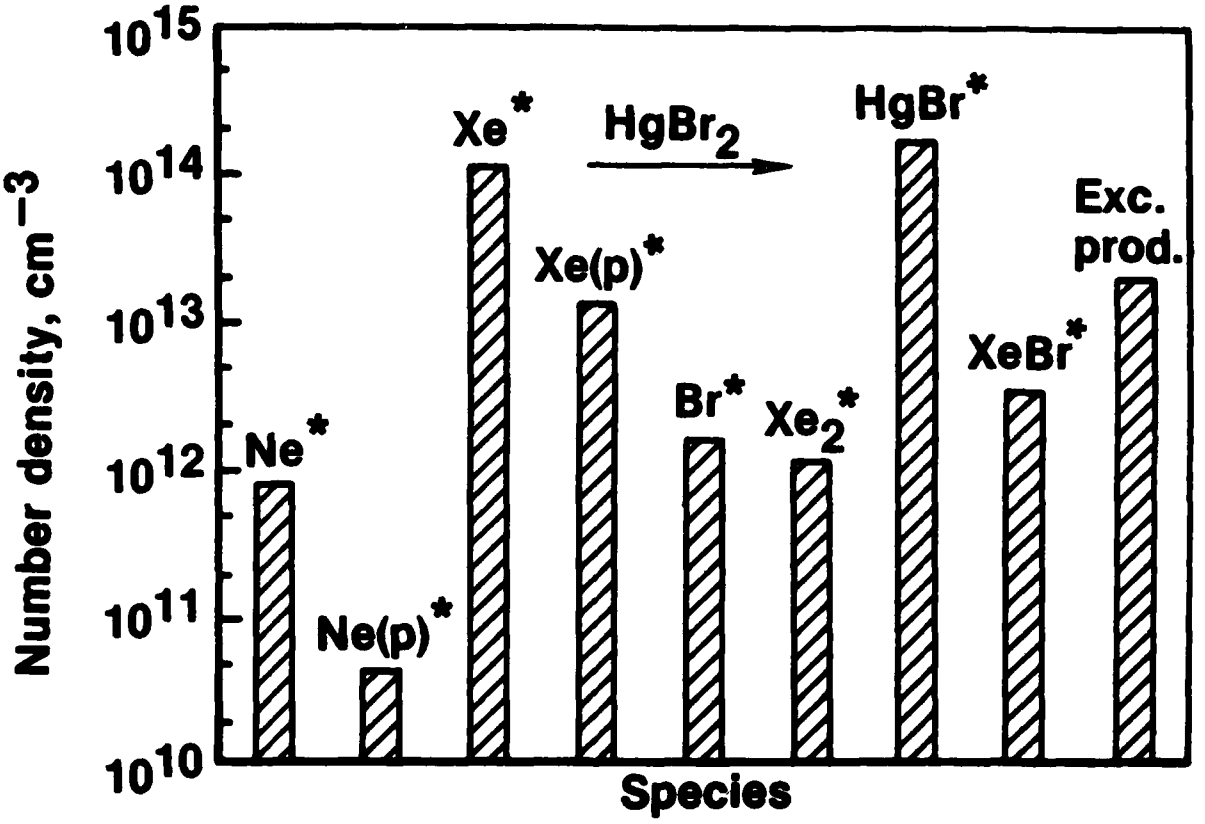

Figure 12. Computed quasi-steady excited state concentrations for the e-beam controlled HgBr(B)/$HgBr_2$ dissociation laser discharge conditions of Table II.

Calculations indicate that the HgBr(B) formation efficiency via this excitation transfer reaction is in the 15-20% range for the conditions of Fig. 12, and that the gain is approximately 4% cm^{-1} (Table II). Reflecting the lower electron density, Fig. 12 also shows that the $Xe^*(p)$ concentration is lower relative to that of $Xe^*(s)$ than is the case in the XeCl laser. The relatively small concentration of $XeBr^*$ indicated in Fig. 12 is a consequence of Xe^+ and Xe_2^+ recombination with Br^- (Flannery, 1981), while the concentration of unspecified excited products indicated results primarily from electron and Br^- recombination reactions involving $HgBr_2^+$.

C. Halogen Dissociation

For the relatively high pressure-high ion density conditions typical of e-beam controlled XeCl and HgBr laser discharges, characteristic excitation and ionization times are much less than the discharge/laser pulse duration. Thus, medium kinetic processes are essentially quasi-steady for most commonly encountered conditions. However, this does not imply that important temporal changes are not occurring. Indeed, it is clear from the previous discussion that the principal reactions resulting directly and indirectly in laser molecule formation involve dissociation of the halogenated species. Additionally, recombination of the dissociation fragments does not occur on the microsecond (or less) time typical of the pulse duration. Thus, since virtually all aspects of discharge/laser characteristics are sensitive to halogen reactions, the properties of the medium typically change significantly throughout the pulse, albeit in a quasi-steady manner.

Figures 13 and 14 present the computed temporal evolution of HCl and $HgBr_2$ dissociation fragments for the XeCl and HgBr laser conditions discussed previously. In both cases the dissociation products are shown to reach levels above 10^{16} cm^{-3} after a few hundred nanoseconds*, a value much higher than the concentrations of all excited and/or ionic species. For the pressures typical of these lasers there is little doubt that both positive and negative cluster ion species involving the dissociation products will be formed (Wiegand, 1981). Other ion rearrangement and/or charge exchange reactions are likely, involving especially the chemically active H atom in XeCl lasers, and the easily ionized molecular fragment HgBr (I.P. $\sim$ 9.0 eV) in $HgBr_2$ dissociation lasers. The success of laser modeling, which generally does not include such reactions, suggests that the primary effect of dissociation is simply loss of the original halogen fuel. Nonetheless, depending on conditions, there are several aspects of laser/discharge behavior that are only partially understood, which may be influenced significantly by reactions involving the products of halogen dissociation. Such effects are most likely to be of significance for repetitive pulse, closed gas flow cycle operation, an area for which there is very little experience.

D. Rare-Gas P-State Processes

As a consequence of the importance of excimer lasers, interest in electronically excited species, particularly the lowest excited states of the rare

* In fast pulse electric discharge lasers, which are pumped more intensely, such changes occur on a much shorter time scale.

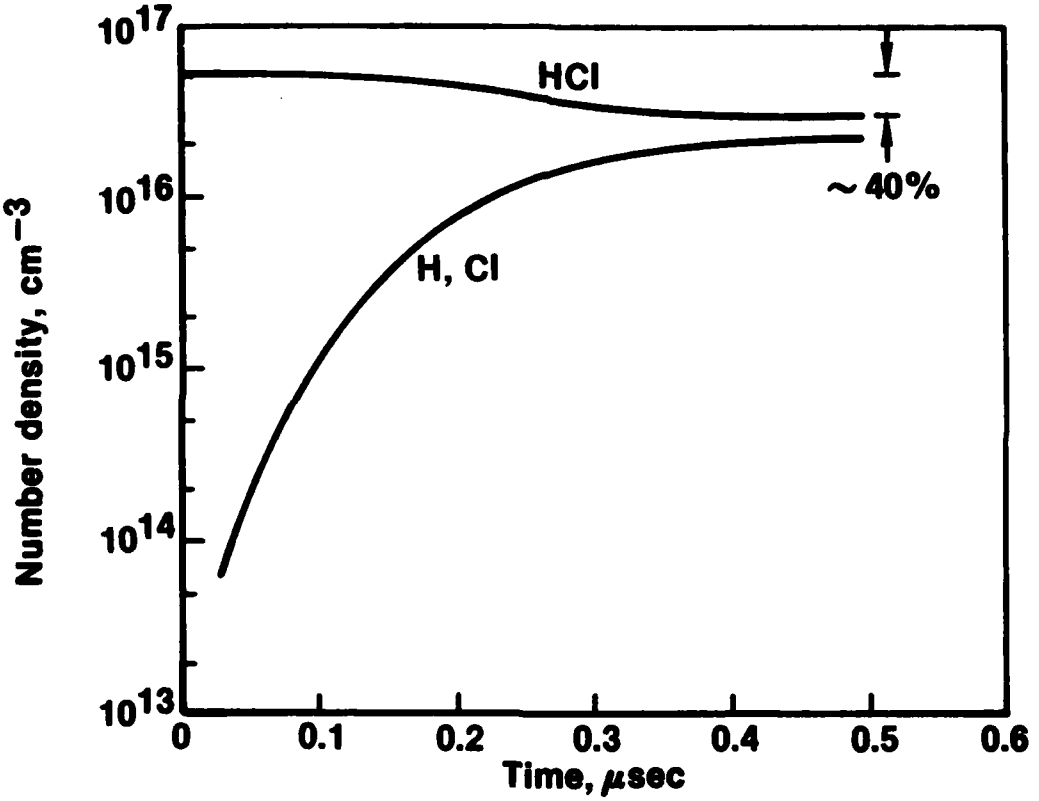

Figure 13. Computed temporal variation of the HCl dissociation products for the XeCl laser conditions of Figs. 9 and 10.

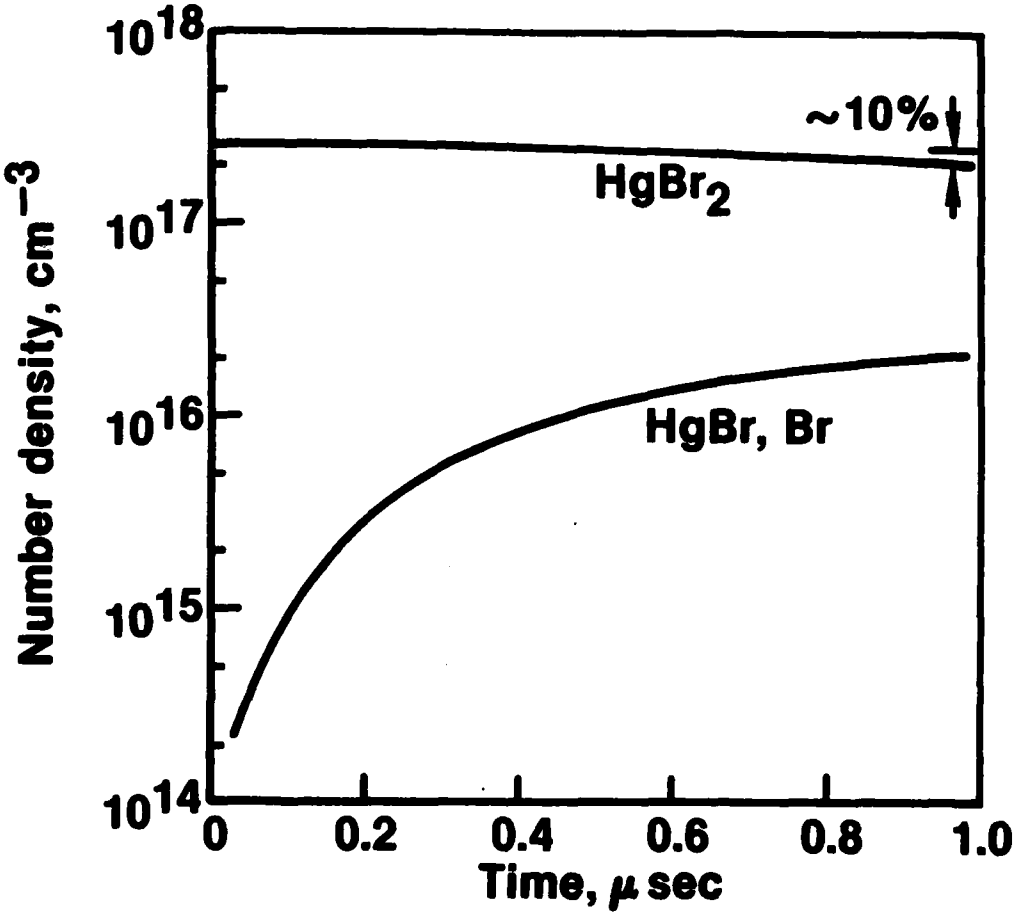

Figure 14. Computed temporal variation of the $HgBr_2$ dissociation products for the HgBr(B)/$HgBr_2$ laser conditions of Figs. 11 and 12.

gases, has been intense. The physical similarities between the rare-gas metastable atoms and alkali metal atoms have significant implications for the laser applications of current interest (Velazco, et al, 1978). One such similarity is very large low energy electron cross section for excitation from the rare-gas s states to the next higher energy manifold of p stress (Hyman, 1978). For rare-gas s state fractional populations greater than about 10^{-5} the resulting electron energy loss is significant (Nighan, 1978a). Additionally, since ionization and photoabsorption from the p states is substantially greater than from the s states (Hyman, 1978, 1979, Duzy and Hyman, 1980), the resultant effects of p state processes on both discharge and laser properties can be quite important (Nighan, 1978a). For these reasons, knowledge of the dominant factors controlling p state population levels in rare-gas mixtures common to both rare-gas and mercury-halide lasers is of considerable importance.

Presented in Fig. 15 is a simplified energy level diagram typical of the rare-gases, which shows the approximate energy relationship between the s and p groups of states, and indicates the processes coupling the groups together. On the basis of energy defect arguments alone, collisional deactivation of states of the p state manifold to the s states, resulting from collisions with ground state rare-gas atoms, would not be expected to be significant. However, Setser and coworkers have recently shown that such intermultiplet energy transfer between rare-gas p and s states occurs by way of complex mechanisms involving curve crossings, in which attractive

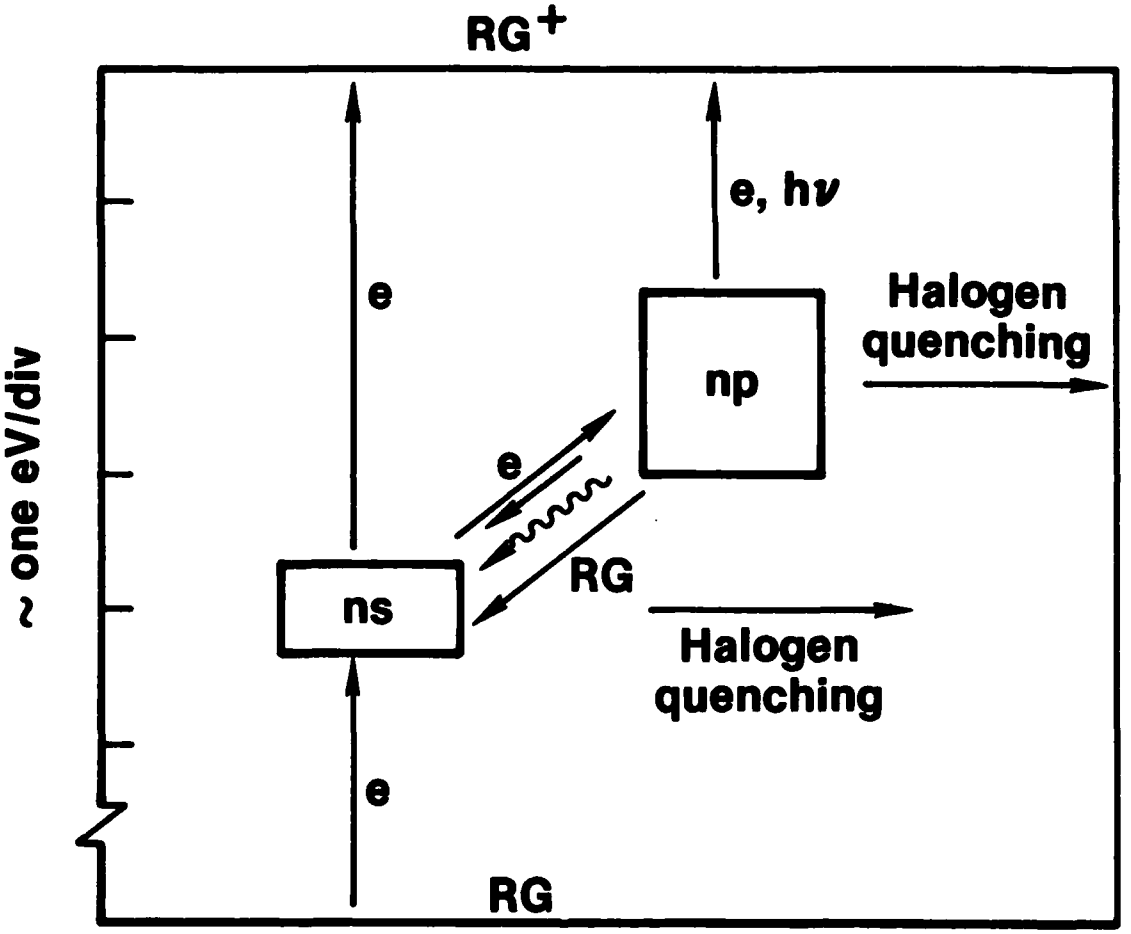

Figure 15. Illustration of the approximate energy relationship and production and loss processes for rare gas s and p state atoms.

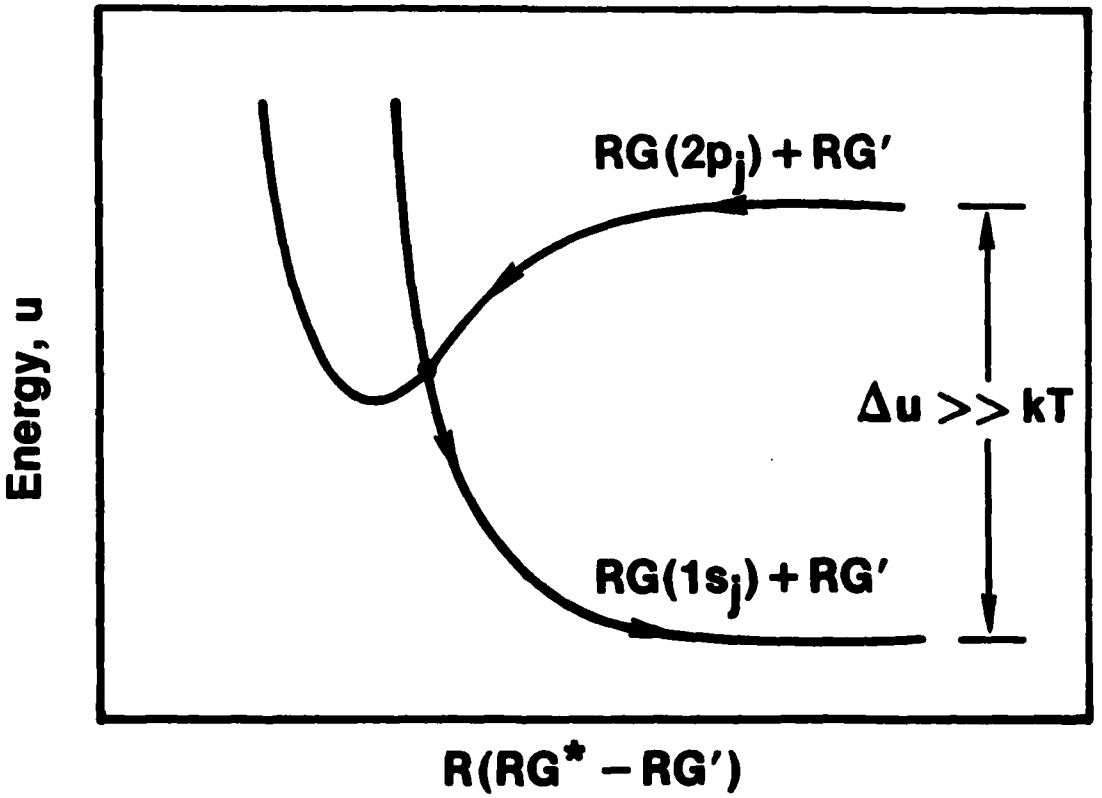

Figure 16. Illustration of rare gas intermultiplet $2p_j$-$1s_j$ deactivation by collisions with ground state rare gas atoms (Chang and Setser, 1978).

bound RG_2^* potential curves from RG and RG(p) interact with the repulsive curves from RG and RG(s) (Chang and Setser, 1978, 1980; Chang, et al, 1980; and Horiguchi, et al, 1981). This sequence of events is illustrated in simplified form in Fig. 16. The rate constants for intermultiplet transfer of this type depend on the specific $2p_j$ levels and on gas mixture. However, effective rate constants for relaxation of the p manifold to the s manifold have been found to be on the order of 1.0×10^{-11} sec^{-1} cm^3 for the rare gases and certain rare-gas mixtures. Thus, at the high pressures typical of rare-gas and mercury-halide lasers, the characteristic time for p → s deactivation by collisions with rare-gas atoms can be as short as 1 nsec. In any case, modeling of laser characteristics has shown that this interesting relaxation mechanism usually controls the population of the p state manifold, thereby exerting an important influence on laser/discharge properties (Nighan, 1978a; and Nighan and Brown, 1980).

V. SUMMARY

The advent of the rare-gas halide laser in 1975 represented a dramatic breakthrough in the ten-year quest for a short wavelength laser having an efficiency and scalability comparable to the IR CO_2 laser. Although a scant five years have passed since the discovery of the rare gas-halide laser, developments in this area have evolved at an extremely rapid pace, propelled by significant advances in understanding of excited state chemistry, electron-halogen attachment, discharge physics, and by the development of sophisticated computer models of laser/discharge properties.

Recently research attention has been directed toward important practical considerations such as volumetric and surface chemistry and the resultant implications on laser short-term temporal behavior and on overall laser system lifetime. For this reason the XeCl(B)/(Xe-HCl) laser operating at 308 nm or Raman shifted to longer wavelengths (Trainor, et al, 1980; Burnham and Djeu, 1978), and the blue/green HgBr(B)/$HgBr_2$ dissociation laser at 502 nm have emerged as leading canidates for a wide range of applications. Both lasers have exhibited favorable chemical characteristics and have demonstrated the potential for repetitive pulse, long-life operation. Additionally, the dominant processes in these lasers have been identified and, although data for certain reactions are still lacking, the general characteristics of XeCl and HgBr lasers operating in a laboratory environment can be predicted in a reasonably satisfactory way. However, there is essentially no information on the effect of HCl or $HgBr_2$ dissociation fragments on excited state or ionic processes in the XeCl and HgBr lasers, respectively. Since the concentration of dissociation products often becomes comparable to that of the parent molecule during the discharge pulse, there is little doubt that their presence will influence discharge/laser properties, especially in closed gas-flow cycle operation. Clearly, a significantly improved understanding of the role of discharge generated neutral species is required.

One of the most significant factors in the emergence of both the XeF and XeCl lasers as efficient UV sources was recognition of the critical role of transient absorption at UV wavelengths by discharge produced species

such as the rare-gas dimer ions. Surprisingly, very little is known about the visible absorption characteristics of the discharge produced excited and ionic species typical of mercury-halide lasers such as HgBr, or of the Xe_2Cl triatomic rare-gas halide laser. Past experience with the UV rare gas-halides strongly suggests that absorption at visible wavelengths will have an important effect on the optical extraction efficiency of such lasers. For this reason it is probable that knowledge of the 400 - 600 nm absorption cross sections for the ionic and excited species known to be present (e.g., Figs. 11 and 12) will lead to a rethinking of the importance of various mixture constituents in visible wavelength lasers, followed by improvements in optical extraction efficiency.

ACKNOWLEDGMENTS

It is a pleasure to acknowledge the contributions to this work of my United Technologies colleagues R. T. Brown, H. H. Michels, L. A. Newman, and W. J. Wiegand, and also those of D. W. Setser of Kansas State University. The expert assistance of L. V. Bromson with the programming and numerical work is also much appreciated, as is the continued interest and support of R. H. Bullis, E. Snitzer and A. J. DeMaria. In addition, the support of the Office of Naval Research is gratefully acknowledged.

REFERENCES

Allan, M. and Wong, S. F. (1981). J. Chem. Phys. (in press).

Azria, R., Roussier, L., Paineau, R. and Tronnc, M. (1974). Rev. Phys. Appl. 9, 469-473.

Brau, C. A. (1979). In "Excimer Lasers" (C. K. Rhodes, ed.) Topics in Applied Physics, Vol. 30, pp. 87-133. Springer-Verlag, New York.

Brewer, L. (1950). In "Excimer Lasers" (C. K. Rhodes, ed.) Topics in Applied Physics, Vol. 30, pp. 87-133. Springer-Verlag, New York.

Brown, R. T. and Nighan, W. L. (1978). Appl. Phys. Lett. 32, 730-733.

Brown, R. T. and Nighan, W. L. (1980). Appl. Phys. Lett. (in press).

Burnham, R. and Djeu, N. (1978). Opt. Lett. 3, 215-.

Champagne, L. F. (1978). Appl. Phys. Lett. 33, 523-525.

Champagne, L. F. (1981). In "Applied Atomic Collision.Physics" (H. S. W. Massey, E. W. McDaniel, and B. Bedserson, eds) Vol. X Gas Lasers, pp.xxx. Academic Press, New York.

Chang, R. S. F., and Setser, D. W. (1978). J. Chem. Phys. 69, 3885-3897.

Chang, R. S. F., and Setser, D. W. (1980). J. Chem. Phys. 72, 4099-4110.

Chang, R. S. F., Horiguchi, H., and Setser, D. W. (1980). J. Chem. Phys. (in press).

Chang, R. S. F. and Burnham, R. (1980). Appl. Phys, Lett. 36 (397-400).

Chantry, P. J. (1981). In "Applied Atomic Collision Physics" (H. S. W. Massey, E. W. McDaniel, and B. Bederson, eds.), Vol. X Gas Lasers, pp. xxx. Academic Press, New York.

Daugherty, J. D. (1976). In "Principles of Laser Plasmas" (G. Bekefi, ed.) pp. 369-419, Wiley, New York.

Duzy, C., and Hyman, H. (1980). Phys. Rev. A (in press).

Elliott, C. J., and Greene, A. E. (1976). J. Appl. Phys. 47, 2946-2953.

Flannery, M. R. (1979). In. J. Quantum Chem: Sumposia 13, 501-429.

Flannery, M. R. (1981). In "Applied Atomic Collision Physics" (H. S. W. Massey, E. W. McDaniel, and B. Bederson, eds.) Vol. X Gas Lasers, pp.xxx. Academic Press, New York.

Gower, M. C., Kearsley, A. J. and Webb, C. E. (1980). IEEE J. Quantum Electron QE-16, 231-234.

Haas, R. A. (1981). In "Applied Atomic Collision Physics" (H. S. W. Massey, E. W. McDaniel, and B. Bederson, eds.), Vol. X Gas Lasers, pp. xxx. Academic Press, New York.

Horiguchi, H., Chang, R. S. F., and Setser, D. W. (1981). J. Chem. Phys. (in press).

Hyman, H. (1977). Appl. Phys. Lett. 31, 14-15.

Hyman, H. (1978). Phys. Rev. A 18, 441-446.

Hyman, H. (1979). Phys. Rev. A 20, 855-859.

Jacob, J. (1981). In "Applied Atomic Collision Physics" (H. S. W. Massey, E. W. McDaniel, and B. Bederson, eds.), Vol. X Gas Lasers, pp.xxx. Academic Press, New York.

Johnsen, R., and Biondi, M. A. (1981). J. Chem. Phys. (in press).

Kolts, J. H., Velazco, J. E., and Setser, D. W. (1979). J. Chem. Phys. 71, 1247-1263.

Long, W. H. (1979). J. Appl. Phys. 50, 168-172.

McCusker, M. (1979). In "Excimer Lasers" (C. K. Rhodes, ed.) Topics in Applied Physics Vol. 30, pp. 47-86. Springer-Verlag, New York.

McKee, T. J., James, D. J., Nip, W. S., Weeks, R. W., and Willis, C. (1980) Appl. Phys. Lett. 36, 943-945.

Miller, J. L., Dickie, J., Davin, J., Swingle, J., and Kan T. (1979) Appl. Phys. Lett. 35, 912-914.

Michels, H. H. Hobbs, R. H., and Wright, L. A. (1979a). J. Chem. Phys. 71, 5053-5062.

Michels, H. H., Hobbs, R. H., and Wright, L. A. (1979b). Appl. Phys. Lett. 35, 153-155.

Morgan, W. L., and Szoke, A. (1981). Phys. Rev. A (in press).

Nighan, W. L. (1970). Phys. Rev. A2, 1989-2000.

Nighan, W. L. (1977a). Phys. Rev. A 15, 1701-1720.

Nighan, W. L. (1977b). Phys. Rev. A 16, 1209-1223.

Nighan, W. L. (1978a). IEEE J. Quantum Electron, QE-14, 714-726.

Nighan, W. L. (1978b). Appl. Phys. Lett. 32, 297-300.

Nighan, W. L. (1980). Appl. Phys. Lett. 36, 173-175.

Nighan, W. L., and Brown, R. T. (1980). Appl. Phys. Lett 36, 498-500.

Parks, J. (1977a). Appl. Phys. Lett. 31, 192-194.

Parks, J. (1977b). Appl. Phys. Lett. 31, 297-300.

Parks, J. (1981). In "Applied Atomic Collision Physics" (H. S. W. Massey, E. W. McDaniel, and B. Bederson, eds.), Vol. X Gas Laers, pp.xxx. Academic Press, New York.

Rohr, K., and Linder, F. (1976). J. Phys. B: Atom. Molec. Phys. 9, 2521-2536.

Rokni, M., Mangano, J. A., Jacob, J. H., and Hsia, J. C. (1978). IEEE J. Quantum Electron. QE-14, 464-481.

Rokni, M., and Jacob, J. A. (1981). In "Applied Atomic Collision Physics" (H. S. W. Massey, E. W. McDaniel, and B. Bederson, eds.), Vol. X Gas Lasers, pp. xxx. Academic Press, New York.

Rothe, D. E. (1969), Phys. Rev. 177, 93-99.

Roxlo, C., and Mandl, A. (1980). J. Chem. Phys. 72, 541-543.

Schulz, G. (1976). In "Principles of Laser Plasmas" (G. Bekefi, ed.) pp.33-38, Wiley, New York.

Schimitschek, E. J., Celto, J. E., and Trias, J. A. (1977). Appl. Phys. Lett. 31, 608-610.

Schimitschek, E. J., and Celto, J. E. (1978). Opt. Lett. 2, 64-66.

Schimitschek, E. J., and Celto, J. E. (1980). Appl. Phys. Lett. 36, 176-178.

Tang, K. Y., Lorents, D. C., Sharpless, R. L., and Huestis, D. L. (1981), Appl. Phys. Lett. (in press).

Tittel, F. K., Wilson, W. L. Stickel, R. E. Marowsky, G., and Ernst, W. E. (1980). Appl. Phys. Lett. 36, 405-407.

Trainor, D. W. Hyman, H., Itzhan, I., and Heinrichs, R. M. (1980). Appl. Phys. Lett. 37, 440-442.

Velazco, J. E., Kolts, J. H. and Setser, D. W. (1978). J. Chem. Phys. 69, 4357-4373.

Wadt, W. (1980). J. Chem. Phys. 72, 2469-2478.

Wiegand, W. J., and Boedeker, L. R. (1980). Appl. Phys. Lett. (in press).

Wiegand, W. J. (1981) In "Applied Atomic Collision Physics" (H. S. W. Massey, E. W. McDaniel and B. Bederson, eds.) Vol. X Gas Lasers, pp.xxx. Academic Press, New York.

Wren, D. J., and Setser, D. W. (1981). J. Chem. Phys. (in press).

APPENDIX

REPRINTS OF RECENTLY PUBLISHED PAPERS

- "Kinetic Processes in the Electrically Excited Mercury-Bromide Dissociation Laser", W. L. Nighan. Applied Physics Letters, Vol. 36, pp. 173-175, pp. 714-726.
- "Efficient XeCl(B) Formation in an Electron-Beam Assisted Xe/HCl Laser Discharge", W. L. Nighan and R. T. Brown. Applied Physics Letters, Vol. 36, pp. 498-520, 1 April 1980.
- "Efficient HgBr(B → X) Laser Oscillation in Electron-Beam Controlled Discharge Excited Xe/$HgBr_2$ Mixtures", R. T. Brown and W. L. Nighan. Applied Physics Letters, Vol. 37, pp. xxx, 15 Dec 1980.

Kinetic processes in the electrically excited mercuric-bromide dissociation laser

William L. Nighan
United Technologies Research Center, East Hartford, Connecticut 06108

(Received 26 September 1979; accepted for publication 19 November 1979)

This letter reports the results of an analysis of basic kinetic and plasma processes in fast-pulse (~100 nsec) electric discharges containing mixtures of the mercuric-bromide molecule, $HgBr_2$, and N_2 in a Ne background. Formation of the laser molecule HgBr ($B\,^2\Sigma^+$) is shown to occur as a result of dissociative excitation transfer following quenching of N_2 ($A\,^3\Sigma_u^+$) by $HgBr_2$.

PACS numbers: 42.55.Hq, 52.20.Hv, 82.30.Eh,

Excitation of the mercury-bromide $B\,^2\Sigma^+ \rightarrow X\,^2\Sigma^+$ laser transition at 502 nm has been achieved by dissociative excitation of the mercuric-bromide molecule $HgBr_2$ in an electric discharge.[1,2] Electrical-optical energy conversion efficiency in the 0.1–1.0% range has been obtained, suggesting that for optimized conditions, efficiency in excess of 1% may be achievable. Moreover, the required concentration of $HgBr_2$ (~2 Torr) can be produced at a temperature (~150 °C) substantially lower than that typical of mercury-halide lasers using mercury-vapor–halogen mixtures. In this letter basic kinetic processes occurring in this new class of mercury-halide lasers will be examined.

Experimentation[1,2] using fast-pulse (~100 nsec) electric discharge excitation indicates an optimum $HgBr_2$ fractional concentration in the 0.2–0.3% range with Ne (or He) serving as the buffer gas at a pressure near 1 atm. Addition of approximately 2–10% N_2 to this mixture has been found to improve laser power and efficiency significantly. For this reason, analysis of HgBr($B\,^2\Sigma^+$) formation kinetics in the N_2 laser mixture has been emphasized in the present study. Electron-N_2 collision processes are expected to dominate discharge processes in the $HgBr_2$-N_2-Ne mixture because of the large N_2 : $HgBr_2$ concentration ratio, the numerous N_2 vibrational and electronic levels having large cross sections, and the high-energy threshold for electronic excitation of Ne. Indeed, the present calculations of electron energy distributions and electron-molecule energy transfer rates for the E/n range typical of the experiments of Refs. 1 and 2 show that over 95% of the total discharge energy is consumed by N_2 vibrational and electronic excitation in approximately equal proportions. Recent measurements have shown that the rate coefficient for dissociative excitation transfer from $N_2(A\,^3\Sigma_u^+)$ to $HgBr_2$ is large,[3] and that the cross section for direct electron dissociative excitation of $HgBr_2$ leading to HgBr($B\,^2\Sigma^+$) is small.[4] These findings are consistent with the HgBr($B\,^2\Sigma^+$) formation sequence illustrated in Fig. 1.

Figure 1 shows the principal N_2 states excited directly by electron impact on ground state N_2. The shaded area refers to the $N_2(B\,'^3\Sigma_u^-)$, $(a'^1\Sigma_u^-)$, $(a^1\Pi_g)$, and $(w^1\Delta_u)$ group of states; and the percentages shown refer to the fractional electron energy initially transferred to each state (or group of states), computed for the experimental conditions of present interest.[1,2] There are numerous $HgBr_2$ electronic states in the 4–10-eV range.[5] In this figure, the regions labeled *a–d* refer to the experimentally determined photoabsorption bands of $HgBr_2$.[1,5] Available evidence indicates that only states in the *b* band, and particularly $HgBr_2(^3\Sigma_u^+)$ and $(^1\Sigma_u^+)$, predissociate to form HgBr($B\,^2\Sigma^+$).

Measurements[3] of $N_2(A\,^3\Sigma_u^+)$ quenching by $HgBr_2$ yield a rate coefficient of 1.0×10^{-10} sec^{-1} cm^3 for the formation of $HgBr(B\,^2\Sigma_u^+)$, and a total quenching coefficient of approximately 3.0×10^{-10} sec^{-1} cm^3, indicative of a branching ratio of about one-third. However, Fig. 1 shows that only 10% of the electron energy is transferred directly to $N_2(A\,^3\Sigma_u^+)$. Thus, a primary consideration in analysis of HgBr($B\,^2\Sigma^+$) formation kinetics in the $HgBr_2/N_2$ system is the ultimate redistribution of the large fraction (~40%) of the discharge energy initially deposited in higher N_2 electronic levels, particularly the coupled $B\,^3\Pi_g$ and $W\,^3\Delta_u$ states which are populated by electron impact and by cascade from higher levels. Under laser discharge conditions, excitation transfer from these states to $HgBr_2$ is likely to occur in a time less than that required for either electronic relaxation to high vibrational levels of $N_2(A\,^3\Sigma_u^+)$, or for vibrational relaxation of the $A\,^3\Sigma_u^+$ state. Michels[6] has carried out an analysis based on consideration of the energy defect corresponding to various N_2^*-$HgBr_2$ collision channels, and on correlations of the spin and symmetry of reaction products. This analysis shows that excitation transfer from $N_2(A\,^3\Sigma_u^+)$ results in the formation of $HgBr_2(^3\Sigma_u^+)$, which correlates diabatically with the HgBr($B\,^2\Sigma^+$) laser state, with some branching to HgBr($A\,^2\Pi$) and HgBr($X\,^2\Sigma^+$) also probable. This conclusion is consistent with measure-

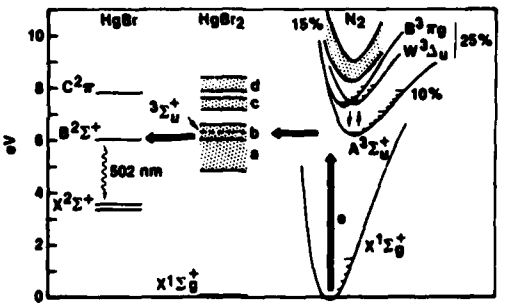

FIG. 1. Simplified energy level diagram illustrating the HgBr($B\,^2\Sigma^+$) formation sequence in electrically excited mixtures of $HgBr_2$ and N_2. The percentages shown refer to the fractional electron energy transfer to each state.

 0003-6951/80/030173-03$00.50

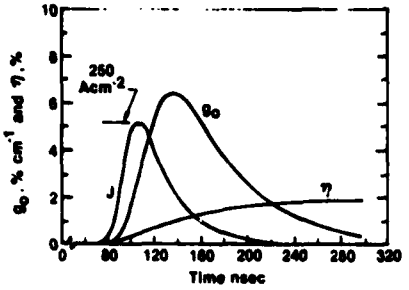

FIG. 2. Temporal variations of discharge current density, zero-field gain (assuming no lower laser level population), and HgBr($B^2\Sigma^+$) formation efficiency computed for a Ne-N_2-$HgBr_2$ mixture in the proportions 0.95 : 0.05 : 0.0025 at a pressure of 1.3 atm and conditions otherwise similar to the experiments of Ref. 1.

ments[3] of $N_2(A^3\Sigma_u^+)$ quenching by $HgBr_2$. In contrast to this situation, excitation transfer from $N_2(W^3\Delta_u)$ leads to $HgBr_2(^3\Delta_u)$, and subsequently to HgBr ($A^2\Pi$) and HgBr($C^2\Pi$), with no branching to HgBr($B^2\Sigma_u^+$). In addition, excitation transfer from $N_2(B^3\Pi_g)$ leads to $HgBr_2(^3\Pi_g)$, which correlates diabatically with the HgBr($C^2\Pi$) state, with branching to the $A^2\Pi$, $B^2\Sigma^+$, and $X^2\Sigma^+$ states of HgBr also possible. Thus, excitation transfer to $HgBr_2$ from the coupled $B^3\Pi_g$ and $W^3\Delta_u$ states of N_2 is expected to result in states of $HgBr_2$ which, for the most part, do not dissociate to produce the HgBr($B^2\Sigma^+$) laser state. In the present analysis, the total rate coefficient for quenching of $N_2(B^3\Pi_g)$ and $N_2(W^3\Delta_u)$ was taken to be the same as the value measured for $N_2(A^3\Sigma_u^+)$, but branching to HgBr($B^2\Sigma^+$) was assumed to be zero.

Because N_2 cross sections for vibrational and electronic excitation are well known, electron energy distributions and related rate coefficients could be calculated reliably for use as input in a self-consistent model of the time-dependent variation of electron, ion, and excited state processes for conditions typical of the fast-pulse discharge experiments of Refs. 1 and 2. For a Ne-N_2-$HgBr_2$ mixture in the proportions 0.95 : 0.05 : 0.0025 at a pressure of 1.3 atm, the measured[1] E/n value at which breakdown occurred was found to be approximately 3×10^{-16} V cm^2, subsequently decreasing to zero in about 150 nsec. For these conditions the present calculations show that the dominant contributions to ionization are Penning ionization of N_2 and $HgBr_2$ by Ne* (~50%), direct electron impact ionization of N_2 (~35%), and direct electron impact ionization of $HgBr_2$ (~15%).[7] Ionization from the highly populated $N_2(A^3\Sigma_u^+)$, $(B^3\Pi_g)$, and $(W^3\Delta_u)$ states was found to be unimportant, a reflection of the relatively high ionization potentials of these excited species. This is significant, since cumulative ionization involving electronically excited species is usually a major contributor to the occurrence of ionization instability and subsequently, discharge arcing.[8]

Presented in Fig. 2 are temporal variations of discharge current density, zero-field gain (assuming no lower laser level population), and the energy efficiency of HgBr($B^2\Sigma^+$) formation computed for conditions typical of those of Ref. 1. The HgBr($B^2\Sigma^+$) formation efficiency at any point is simply the time-integrated ratio of the energy flow through the HgBr($B^2\Sigma_u^+$) state to the total energy deposited in the discharge up to that time. Both the peak values and temporal evolution of the computed current density and gain are in good agreement with measured values.[1] For the conditions of this example HgBr($B^2\Sigma^+$) is produced by way of excitation transfer from the $N_2(A^3\Sigma_u^+)$ state alone as discussed previously, the latter produced by direct electron impact of N_2, and to a lesser extent by $N_2(B^3\Pi_g)\rightarrow N_2(A^3\Sigma_u^+)$ transitions resulting from collisions with electrons and N_2 molecules. The primary loss of HgBr($B^2\Sigma^+$) is due to spontaneous decay (~47%), and to collisions with $HgBr_2$ (~17%), Ne (~16%), electrons (~13%) and N_2 (~7%). These processes result in an effective upper level lifetime of about 10 nsec, corresponding to a saturation intensity of approximately 175 kW/cm^2, which is also in good agreement with measured values.[1] Figure 2 indicates that HgBr($B^2\Sigma^+$) formation efficiency reaches a maximum level of about 2.0% by the end of the pulse. Measured[1] laser efficiency under these conditions is typically 0.5%, a value consistent with an overall optical extraction efficiency of 25%.

Figure 3 shows the temporal variation of several major species corresponding to the conditions of Fig. 2. The concentrations of the $N_2(A^3\Sigma_u^+)$ and the coupled $N_2(B^3\Pi_g)$ and $N_2(W^3\Delta_u)$ states reach very high levels at about the time the current density reaches its peak, reflecting the relatively large values of N_2 concentration, electron density, and e-N_2 excitation rate coefficients. These N_2 states decay rather slowly, indicative of their rate of quenching by $HgBr_2$, which is present in small concentration. In the present model the temporal decay of HgBr($B^2\Sigma^+$) essentially follows the $N_2(A^3\Sigma_u^+)$ population as shown in the figure. However, vibrational redistribution within the $N_2(A^3\Sigma_u^+)$ state will occur as a function of time, particularly as the pumping decreases (decreasing n_e and E/n). Indeed, both the total $N_2(A^3\Sigma_u^+)$ quenching rate and $HgBr_2$ product states may actually exhibit a dependence on $N_2(A^3\Sigma_u^+)$ vibrational level, and therefore on time.

Fractional dissociation of $HgBr_2$ reaches a value of approximately 10% for the present example, resulting in a significant concentration of HgBr($X^2\Sigma^+$) by the end of the

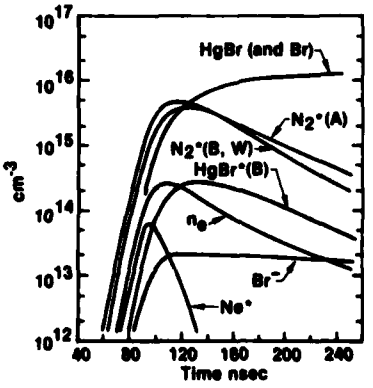

FIG. 3. Temporal variation of selected species concentrations corresponding to the conditions of Fig. 2.

pulse. A significant fraction of $HgBr(X\,^2\Sigma^+)$ is initially produced in the $v = 22$ terminal laser level which is apparently relaxed rather rapidly by collisions with neutrals. However, since the electron density and electron temperature remain relatively high throughout the entire pulse, vibrational excitation of HgBr by electrons may result in a vibrational temperature well above that typical of the gas temperature. Thus, it is probable that lower laser level buildup becomes significant at some time prior to the end of the pulse for the conditions examined here.

Although addition of N_2 to the Ne-$HgBr_2$ mixture results in a significant improvement in pulse energy and efficiency, particularly the former, the $HgBr_2$ dissociation laser does operate at an efficiency above 0.1% without N_2 in the mixture.[1] The present analysis shows that electron energy transfer, ionization, and $HgBr(B\,^2\Sigma^+)$ formation processes are completely different in the absence of N_2. Calculations indicate that in Ne-$HgBr_2$ mixtures, the dominant electron energy transfer processes are Ne metastable production followed by Penning ionization of $HgBr_2$, and direct electron impact ionization of $HgBr_2$.[7] Predissociating states of $HgBr_2$ can be produced either by the ion-ion recombination reaction, $HgBr_2^+ + Br^- + Ne \rightarrow HgBr_2^* + Br + Ne$, or by electron-ion recombination, $HgBr_2^+ + e \rightarrow HgBr_2^*$. Based on estimates for ion loss rates,[9] the present calculations show that ion loss due to electron-ion recombination is 5–10 times larger than that due to ion-ion recombination. Since numerous excited states of $HgBr_2$ can be formed by either recombination reaction, the branching ratio for $HgBr(B\,^2\Sigma^+)$ formation is not likely to be very high. By assuming a branching ratio of 0.2 for $HgBr(B\,^2\Sigma^+)$ formation via recombination reactions, values of peak gain ($\sim 4\%$ cm^{-1}) and $HgBr(B\,^2\Sigma^+)$ formation efficiency ($\sim 1.75\%$) were computed for conditions generally similar to those of Fig. 2. These values are somewhat less than those typical of mixtures containing N_2, a result consistent with experimental observations.[1] However, for similar current density levels the total energy deposited in the gas is significantly less in the absence of N_2, reflecting substantially lower E/n levels typical of Ne-$HgBr_2$ mixtures. It should also be pointed out that with N_2 in the mixture, recombination reactions are insignificant compared to $N_2(A\,^3\Sigma_u^+)$ excitation transfer insofar as $HgBr(B\,^2\Sigma^+)$ formation is concerned.

Although the data base required for comprehensive modeling of mercuric-bromide dissociation lasers is far from complete, the present analysis shows that available experimental observations can be interpreted in a self-consistent manner for $HgBr_2$ laser mixtures containing N_2. Analysis of $HgBr(B\,^2\Sigma^+)$ formation kinetics and discharge characteristics indicate that the $HgBr_2/N_2$ system has considerable potential for efficient scaling to energy levels substantially in excess of those reported to date.

The author acknowledges numerous helpful discussions with his colleagues particularly L.A. Newman and H.H. Michels. Also, the expert assistance of L. Bromson with the numerical work is much appreciated. Additionally, the author thanks E.J. Schimitschek and R. Burnham for access to experimental data prior to publication. This work was supported in part by the Office of Naval Research.

[1] E.J. Schimitschek and J.E. Celto, Opt. Lett. 2, 64 (1978); Appl. Phys. Lett. 36, (1980) (to be published).
[2] R. Burnham, Appl. Phys. Lett. 33, 156 (1978).
[3] R.S.F. Chang and R. Burnham (unpublished).
[4] J. Allison and R.N. Zare, Chem. Phys. 35, 263 (1978).
[5] K. Wieland, Z. Phys. 77, 157 (1932); W.R. Wadt, J. Chem. Phys. (to be published).
[6] H.H. Michels (private communication).
[7] For the purpose of the present analysis, the ionization cross section for $HgBr_2$ has been assumed to increase from threshold at 10.6 eV to a peak value of 5×10^{-16} V cm^2 in the 50–100-eV range. The rate coefficient for dissociative attachment of $HgBr_2$ was taken as 1×10^{-10} sec^{-1} cm^3. The results presented in Figs. 2 and 3 were found to be relatively insensitive to variations in the $HgBr_2$ ionization and attachment rate coefficients.
[8] R.T. Brown and W.L. Nighan, Appl. Phys. Lett. 32, 730 (1978).
[9] In this analysis an effective electron-ion recombination coefficient of 1.0×10^{-7} sec^{-1} cm^3 was used for $HgBr_2^+$, along with a value of 3×10^{-7} sec^{-1} cm^3 for the reaction $HgBr_2^+ + Br^- + Ne \rightarrow HgBr_2^* + Br + Ne$, as recently computed by M.R. Flannery (private communication).

Efficient XeCl(B) formation in an electron-beam assisted Xe/HCl laser discharge

William L. Nighan and Robert T. Brown
United Technologies Research Center, East Hartford, Connecticut 06108

(Received 17 December 1979; accepted for publication 15 January 1980)

XeCl(B) formation processes are examined for conditions typical of a discharge-excited laser using HCl as the chlorine donor. It is shown that vibrational excitation of HCl followed by dissociative attachment is a primary step in the reaction sequence resulting in Cl^-. XeCl(B) formation is the result of a three-body Xe^+-CL^- recombination reaction. Experimental results are presented which demonstrate efficient (~2%) XeCl laser operation in an e-beam assisted discharge in which over 75% of the energy was deposited by the discharge.

PACS numbers: 42.55.Hq, 42.60.By

Recently, efficient (~5%) laser oscillation on the XeCl($B \rightarrow X$) transition (308 nm) has been reported using both pure electron-beam excitation[1,2] and an electron-beam controlled discharge.[2] In both cases, the observation of efficient operation with little or no long-term degradation in laser performance is attributed to the use of HCl as the halogen donor.[1-3] However, relatively little is known about HCl reaction kinetics in the XeCl laser medium, a factor which has hampered development of a good understanding of basic proceses in this laser. The present letter addresses this problem, and reports results of an investigation of XeCl(B) formation kinetics and plasma processes in an electron-beam assisted discharge for total volumetric energy loading comparable to that reported previously,[1,2] but under conditions such that electrical energy input was dominated by the discharge.

There are several important features which set HCl apart from other effective halogen donors: (1) a high dissociation energy (4.45 eV), (2) a very high cross section for vibrational excitation by electrons,[4] and (3) a cross section for dissociative attachment from the ground vibrational level which is substantially lower than that of the halogen donors typically used in rare-gas fluoride lasers. Formation of XeCl(B) by way of $Xe(^3P_2)$-HCl reactions is slightly endothermic at 300 °K,[5] reflecting the strong HCl bond energy. Thus the large measured[5] $Xe(^3P_2)$ quenching rate by HCl is apparently a purely dissociative reaction and does not result in formation of the XeCl(B) upper laser level. Although quenching of $Xe(^3P_1, ^3P_0, ^1P_1)$ by HCl may result in XeCl(B) formation, at present there are no data for such reactions. In addition, while the large cross section for HCl vibrational excitation ensures the presence of a high fractional concentration of vibrationally excited HCl in laser plasmas, there is no evidence suggesting efficient XeCl(B) formation by way of $Xe(^3P_2)$-HCl(v) reactions.

A more likely consequence of HCl vibrational excitation is enhanced dissociative attachment. Indeed, our analysis of current-voltage characteristics for electron-beam controlled discharges in a variety of rare-gas–HCl mixtures indicate the occurrence of an electron loss process which increases with time throughout the discharge pulse. Modeling studies show that this enhanced electron loss correlates with the growth in the concentration of vibrationally excited HCl. Further, without taking this effect into account, it is not possible to quantitatively model either discharge characteristics or laser properties in XeCl laser mixtures on the basis of other *known* reactions alone.

Presented in Fig. 1 are the rate coefficients for vibrational excitation and attachment for HCl in the ground vibrational level, computed for a Ne(0.989)-Xe(0.01)-HCl(0.001) laser mixture. The vibrational cross section of Rohr and Linder[4] was used in the calculation, and the shape of the attachment cross section of Ziesel, Nenner, and Schulz[6] was used, adjusted in magnitude to yield a rate coefficient consistent with our experimental observations in vibrationally cold HCl. The shaded region in this figure is indicative of the 10- to 20-fold increase in the *effective* attachment rate of HCl resulting from vibrational excitation, as deduced from the present modeling of the characteristics of rare-gas–HCl discharges.[7] Very recent measurements by Wong[8] indicate an increase of more than an order of magnitude in the attachment cross section due to HCl vibrational excitation, a result that provides additional support for the present conclusions.

On the basis of the interpretation discussed above, it is concluded that vibrational excitation of HCl is a fundamental process in XeCl lasers using HCl as the chlorine donor. For discharge-excited lasers, modeling studies indicate that XeCl(B) formation proceeds by way of the sequence illustrated in Fig. 2. In this sequence, electron energy transfer is

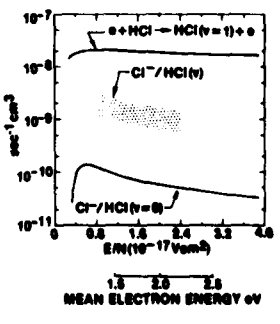

FIG. 1. Rate coefficients for vibrational excitation and dissociative attachment for HCl in the ground vibrational level, computed for a Ne(0.989)-Xe(0.01)-HCl(0.001) laser mixture. The shaded region is indicative of the magnitude of the effective rate coefficient for attachment to vibrationally excited HCl as inferred from the present study.

 0003-6951/80/070498-03$00.50

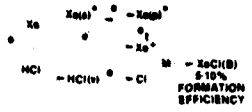

FIG. 2. XeCl(B) formation sequence in discharge-excited Ne-Xe-HCl laser mixtures.

dominated by Xe metastable production and by excitation of metastable atoms to the higher-lying manifold of Xe p states. Production of Xe^+ is found to be a cumulative process in which stepwise ionization of metastable and p-state atoms make comparable contributions. Formation of XeCl(B) results from the three-body recombination of Xe^+ with Cl^-, the latter produced by dissociative attachment to vibrationally excited HCl as discussed previously. Of course, there are numerous energy loss processes interfering with the simplified XeCl(B) formation sequence illustrated in Fig. 2, particularly electron elastic collisions with Ne, Xe($p \rightarrow s$) relaxation by neutral collisions, and dissociative quenching of both Xe metastable and p-state atoms by HCl. Even under optimum laser discharge conditions, these loss processes account for approximately 50% of the discharge energy. Nevertheless, numerical analysis shows that XeCl(B) is produced according to the sequence indicated in Fig. 2 with an efficiency in the 5–10% range for a wide range of discharge conditions.

Because XeCl(B) formation proceeds by way of an ionization-recombination channel, it follows that attainment of a high discharge-to-e-beam-energy-enhancement factor using an e-beam discharge excitation technique requires that only a small fraction of the ionization be provided by the electron beam. In this circumstances, the discharge is e-beam *assisted* rather than e-beam *controlled* as in the case of the KrF laser,[9] for example. Use of an e-beam assisted discharge operating in a quasiavalanche mode for XeCl laser excitation significantly minimizes the burden on the e-beam technology, while providing flexibility and scalability not possible using uv-preionized or corona-preionized fast-pulse discharge excitation. In the present investigation, the e-beam discharge arrangement reported upon previously was utilized.[10] The active volume of this system was $1.5 \times 2.0 \times 50$ cm. Figure 3 shows representative current-voltage characteristics for the laser mixture of Fig. 1 at a total pressure of 3 atm. The discharge was triggered by initiation of a 0.5-μsec electron-beam pulse at a current density level of 1 A cm^{-2}. Following initiation of the e-beam pulse, the applied voltage collapsed from an initial level of approximately 4.5×10^{-17} V cm^2 to a value of about 1.9×10^{-17} V cm^2. The total energy deposited by the discharge in this case was 6.4 J and the energy deposited by the electron beam was 1.1 J, corresponding to a discharge-to-beam-energy-enhancement factor of 6.

As shown in Fig. 3, the onset of the XeCl($B \rightarrow X$) laser pulse occurred approximately 0.15 μsec after the initiation of the discharge current pulse and lasted for 0.35 μsec. Measured laser pulse energy was 0.16 J, corresponding to an intrinsic electrical-optical energy conversion efficiency of about 2%, while measured values of peak gain for these conditions were about 3.1% cm^{-1}. For the e-beam levels and cavity parameters of this experiment, laser oscillation due to the e-beam alone was near the threshold level and often was not discernable at all.

Figure 4 shows computed values of zero-field gain, absorption, XeCl(B) formation efficiency, and discharge-to-e-beam-enhancement factor corresponding to the conditions of Fig. 3. Formation efficiency and enhancement factor are time intgrated. For these conditions the volumetric absorption is dominated by Xe_2^+, and to a lesser extent by Ne_2^+ and CL^-, and is at a level approximately one-tenth that of the gain, consistent with an optical extraction efficiency of about 40%. On this basis, the computed XeCl(B) formation efficiency of 4.5% is in satisfactory agreement with the measured laser efficiency of 2.0%. The computed gain is also in accord with the experimental observation. Figure 4 shows that the integrated energy enhancement factor reaches a value of 10 near the discharge current density maximum, and then declines to about 6. This trend reflects the fact that the electron-beam pulse is sensibly constant for about 0.5 μsec. Thus, as the discharge current and voltage begin to decline after approximately 0.3 μsec, the fractional contribution of the discharge to the total energy deposition decreases. Nevertheless, these results indicate that efficient XeCl($B \rightarrow X$) laser operation should be possible using the e-beam *assisted* discharge technique under conditions such that 90% or

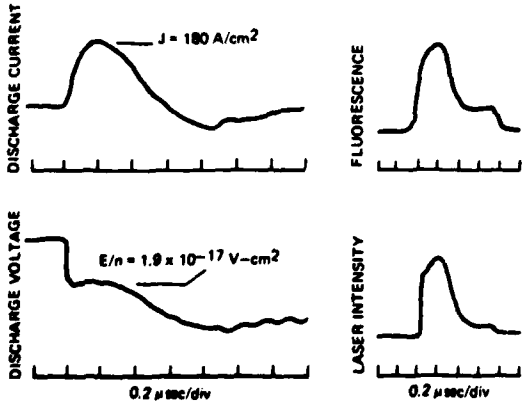

FIG. 3. Representative discharge and XeCl($B \rightarrow X$) laser characteristics in an e-beam assisted laser discharge for the mixture of Fig. 1 at a pressure of 3 atm.

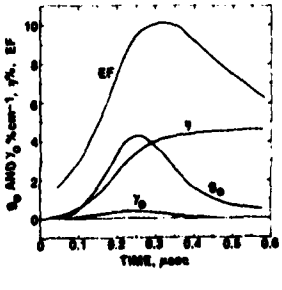

FIG. 4. Computed zero-field gain, absorption, XeCl(B) formation efficiency, and discharge with an e-beam energy enhancemnt factor corresponding to the experimental conditions of Fig. 3. Formation efficiency and enhancement factor are time integrated.

more of the energy is provided by the discharge. This method of XeCl laser excitation significantly reduces the technology problems associated with the *e*-beam portion of the driver, and should provide substantially longer pulse lengths and a measure of scalability not typical of UV-preionized discharge excitation.

The authors wish to thank R. Preisach and L. Bromson for their expert assistance with the experimental and numerical work, respectively, and also acknowledge helpful conversations with A. Herzenberg and S.F. Wong on the topic of HCl dissociative attachment. This work was supported in part by the Naval Ocean Systems Center and by the Office of Naval Research.

[1]L.F. Champagne, Appl. Phys. Lett. **33**, 523 (1978).
[2]D. Rothe, J.B. West, and M.L. Bhaumik, IEEE J. Quantum Electron. QE-**15**, 314 (1979).
[3]R. Burnham, Opt. Commun. **24**, 161 (1978).
[4]K. Rohr and F. Linder, J. Phys. B **9**, 2521 (1976).
[5]J.H. Kolts, J.E. Velazco, and D.W. Setser, J. Chem. Phys. **71**, 1247 (1979).
[6]J.P. Ziesel, I. Nenner, and G.J. Schulz, J. Chem. Phys. **63**, 1943 (1975).
[7]The term "effective attachment coefficient" as used here refers to the average over all HCl vibrational levels for the conditions of the present experiment, i.e., $k_a^{\prime\prime} = [\mathrm{HCl}]^{-1} \Sigma \mathrm{HCl}(v) k_a(v)$.
[8]S.F. Wong, in *Invited Papers of the Symposium on Electron-Molecule Collisions, 1979*, edited by I. Shimamura and M. Matsuzawa.
[9]M. Rokni, J.A. Mangano, J.H. Jacob, and J.C. Hsia, IEEE J. Quantum Electron. QE-**14**, 464 (1978).
[10]R.T. Brown and W.L. Nighan, Appl. Phys. Lett. **32**, 730 (1978); **35**, 144 (1979).

Efficient HgBr(B→X) Laser Oscillation in Electron-Beam Controlled Discharge Excited Xe/$HgBr_2$ Mixtures

By

Robert T. Brown and William L. Nighan

United Technologies Research Center, East Hartford, CT 06108

ABSTRACT

This letter reports results of an investigation of HgBr($B^2\Sigma^+ \rightarrow X^2\Sigma^+$) laser oscillation at 502 nm in Xe-$HgBr_2$ mixtures excited using an electron-beam controlled discharge. Measured values of instantaneous electrical-optical energy conversion efficiency were 2%, a level substantially higher than that typical of N_2-$HgBr_2$ mixtures. Calculations show that efficiencies of 5-10% may be possible under optimized conditions.

The $HgBr(B^2\Sigma^+ \rightarrow X^2\Sigma^+)$ laser operating at 502 nm promises to be an important optical source in the blue/green region of the spectrum. Excitation of this laser transition has been achieved by dissociative excitation of the mercuric-bromide molecule, $HgBr_2$, in an electric discharge[1]. Using N_2-$HgBr_2$ mixtures, electrical-optical energy conversion efficiencies in the 0.5-1.0% range have been obtained[1]. Analysis of the kinetics of electrically excited N_2-$HgBr_2$ mixtures has shown that the $HgBr(B^2\Sigma^+)$ laser molecule is formed following predissociation of $HgBr_2(^3\Sigma_u^+)$, the latter produced as a result of $N_2(A^3\Sigma_u^+)$ quenching by $HgBr_2$ molecules[2]. However, calculations show that the production efficiency of $N_2(A^3\Sigma_u^+)$ in N_2-$HgBr_2$ discharges is about 10-15%; and recent measurements indicate that the $N_2(A^3\Sigma_u^+)$-$HgBr_2$ branching fraction for $HgBr(B^2\Sigma^+)$ formation is only 15-20%[3]. These factors may limit the efficiency of the discharge excited $HgBr(B)/HgBr_2$ dissociation laser to a value of approximately 1% when N_2 is used as the energy transfer molecule.

By way of contrast, recent measurements show that the $Xe(^3P_2)$ metastable atom has a large rate coefficient for $HgBr_2$ dissociative excitation; and that $HgBr(B^2\Sigma^+)$ is formed with near unit efficiency[4]. In addition, the present calculations show that $Xe(^3P_2)$ metastable atoms can be produced with high efficiency (>50%) over a broad range of electric discharge conditions. For these reasons Xe has unusual potential as an energy transfer species in the $HgBr(B)/HgBr_2$ dissociation laser. In this letter we report results of efficient HgBr(B→X) laser oscillation in Xe-$HgBr_2$ mixtures using an electron-beam controlled discharge.

The present experiments were carried out using a 1.5 cm x 1.7 cm x 50 cm active volume within the heated discharge cell shown schematically in Fig. 1. Previous investigations[5] have shown that proper cell design is critical in order

to maintain chemical purity of the gas mixture. In order to keep $HgBr_2$-surface interactions to a minimum, in this cell the only materials in contact with the working gas mixture were type 316 stainless steel, Pyrex, Kalrez and dielectric-coated mirrors. $HgBr_2$ crystals were contained in a Pyrex reservoir positioned in a side-arm as shown in the figure. Variation of the cell (and reservoir) temperature in the 150-200°C range provided a corresponding variation in $HgBr_2$ partial pressure from about one Torr to approximately 15 Torr. The electron-beam system and discharge driver utilized in this investigation have been described previously[6].

Presented in Fig. 2 are representative measured characteristics for a mixture containing 10% Xe in a Ne buffer at a total pressure of 2 atm and a temperature of 185°C. Based on available vapor pressure data[7], the $HgBr_2$ concentration for these conditions was 2.4×10^{17} cm^{-3}, corresponding to a mixture fraction of approximately 0.007. In this case the electron-beam was initiated 200 ns before the discharge voltage and provided a constant e-beam current density of 0.5 Acm^{-2} for 1.2 μsec. The discharge voltage was provided by a low inductance capacitor of a size so as to produce only a very slight decrease in voltage (i.e., E/n) during the pulse. With this arrangement it was possible to produce a highly uniform plasma medium which was essentially quasi-steady. For the conditions of Fig. 2 the measured current and voltage exhibited essentially steady-state behavior for over 0.5 μsec, at which time the discharge was terminated by arcing.

Time-dependent discharge and laser properties were modeled numerically using procedures which have been described previously[2,6]. Computed current-voltage

characteristics were found to be in very good qualitative and quantitative agreement with measured values over a range of E/n values and $HgBr_2$ concentrations. In addition, the onset of arcing could be predicted and was shown to be due to volumetric ionization instability[6]. Prior to the onset of arcing the discharges were found to operate in a high impedance (2-3 ohms), externally controlled mode. Modeling of discharge properties indicated that for conditions typical of this investigation (e.g. Fig. 2) 80-90% of the deposited energy was provided by the discharge, and 60-70% of the ionization was provided by the e-beam, values found to be consistent with experimental observations. Thus, the $Ne/Xe/HgBr_2$ discharges examined in this investigation were e-beam controlled and exhibited a high discharge:e-beam energy enhancement factor.

The $HgBr(B^2\Sigma^+ \rightarrow X^2\Sigma^+)$ fluorescence was found to be a relatively sensitive function of applied voltage, reflecting the strong dependence of $Xe(^3P_2)$ metastable production on E/n. Modeling of discharge characteristics indicated that $HgBr(B^2\Sigma^+)$ was produced with an efficiency typically in the 15-20% range by way of the reaction sequence,

$$e \xrightarrow{Xe} Xe(^3P_2) \xrightarrow{HgBr_2} HgBr(B^2\Sigma^+).$$

Computed zero-field gain based on the calculated $HgBr(B^2\Sigma^+)$ concentration and using a stimulated emission cross section of 2.4×10^{-16} cm^2 was approximately 0.03 cm^{-1} for the conditions of Fig. 2.

Using an internally-mounted optical cavity consisting of a 4.0 m max R mirror and a flat 90% R output coupler, the laser pulse shown in Fig. 2 was obtained. The output beam imaged the full 1.5 cm x 1.7 cm discharge cross section and was found to be very uniform. Although the onset of laser oscillation was delayed, Fig. 2 shows that a uniform laser pulse of almost 400 nsec duration was

obtained. Moreover, the instantaneous electrical-optical energy conversion efficiency was found to be 2.0 percent, a level substantially higher than that typical of $N_2/HgBr_2$ laser mixtures. However, calculations show that in the absence of appreciable volumetric absorption (i.e., for gain/absorption ratios greater than 10) laser efficiencies greater than 5% should be attainable for these conditions. Both the delayed laser onset and the apparently low optical extraction efficiency are suggestive of a net gain lower than the computed value, and/or a relatively high level of volumetric absorption. With an $HgBr_2$ concentration in excess of 10^{17} cm^{-3}, even a low level of surface reactions and/or impurities introduced with the $HgBr_2$ could result in a substantial level of neutral impurities, one or more of which may either absorb at the laser wavelength or quench HgBr(B). Additionally, ionic or excited states of $HgBr_2$ itself may absorb in the blue/green region of the spectrum. These possibilities are presently being studied in more detail.

The present investigation has shown that use of Xe as the primary energy receptor-transfer species in e-beam controlled discharge excited $HgBr(B)/HgBr_2$ dissociation lasers permits laser efficiency substantially higher than reported for N_2-$HgBr_2$ mixtures. More importantly, calculations show that electrically excited Xe-$HgBr_2$ mixtures have the potential for development as blue/green sources with efficiencies even higher than those measured in the present experiments. Modeling of discharge/laser properties for a variety of conditions suggests that electrical-optical energy conversion efficiencies of 5-10% may be possible under optimized conditions.

The authors acknowledge helpful discussions with their UTRC collegues L. A. Newman, W. J. Wiegand and H. H. Michels, and also with D. W. Setser. In addition, the expert assistance of R. Preisach and L. Bromson is greatly appreciated. This work was supported in part by the Naval Ocean Systems Center and by the Office of Naval Research.

REFERENCES

1. E. J. Schimitschek and J. E. Celto: Appl. Phys. Lett. 36, 176 (1980), and references cited therein.
2. W. L. Nighan: Appl. Phys. Lett. 36, 173 (1980).
3. T. D. Dreiling and D. W. Setser: Chem. Phys. Lett. (in press).
4. R. S. F. Chang and R. Burnham: Appl. Phys. Lett. 36, 397 (1980).
5. E. J. Schimitschek and J. E. Celto: Optics Lett. 2, 64 (1978).
6. R. T. Brown and W. L. Nighan: Appl. Phys. Lett. 32, 730, 1978; also Appl. Phys. Lett. 35, 144 (1979).
7. L. Brewer: In The Chemistry and Metallurgy of Miscellaneous Materials. (L.L. Quill, ed.), McGraw-Hill, New York 1950.

FIGURE CAPTIONS

Fig. 1. Illustration of heated HgBr(B)/$HgBr_2$ laser discharge cell.

Fig. 2. Representative characteristics for an e-beam controlled discharge excited mixture comprised of 10% Xe in a Ne buffer at a total pressure of 2 atm and a temperature of 185°C. For these conditions the $HgBr_2$ concentration in the cell was $2.4 \times 10^{17} cm^{-3}$, approximately 0.7% of the total mixture. The e-beam current density (at the center of the discharge) was 0.5 Acm^{-2}.

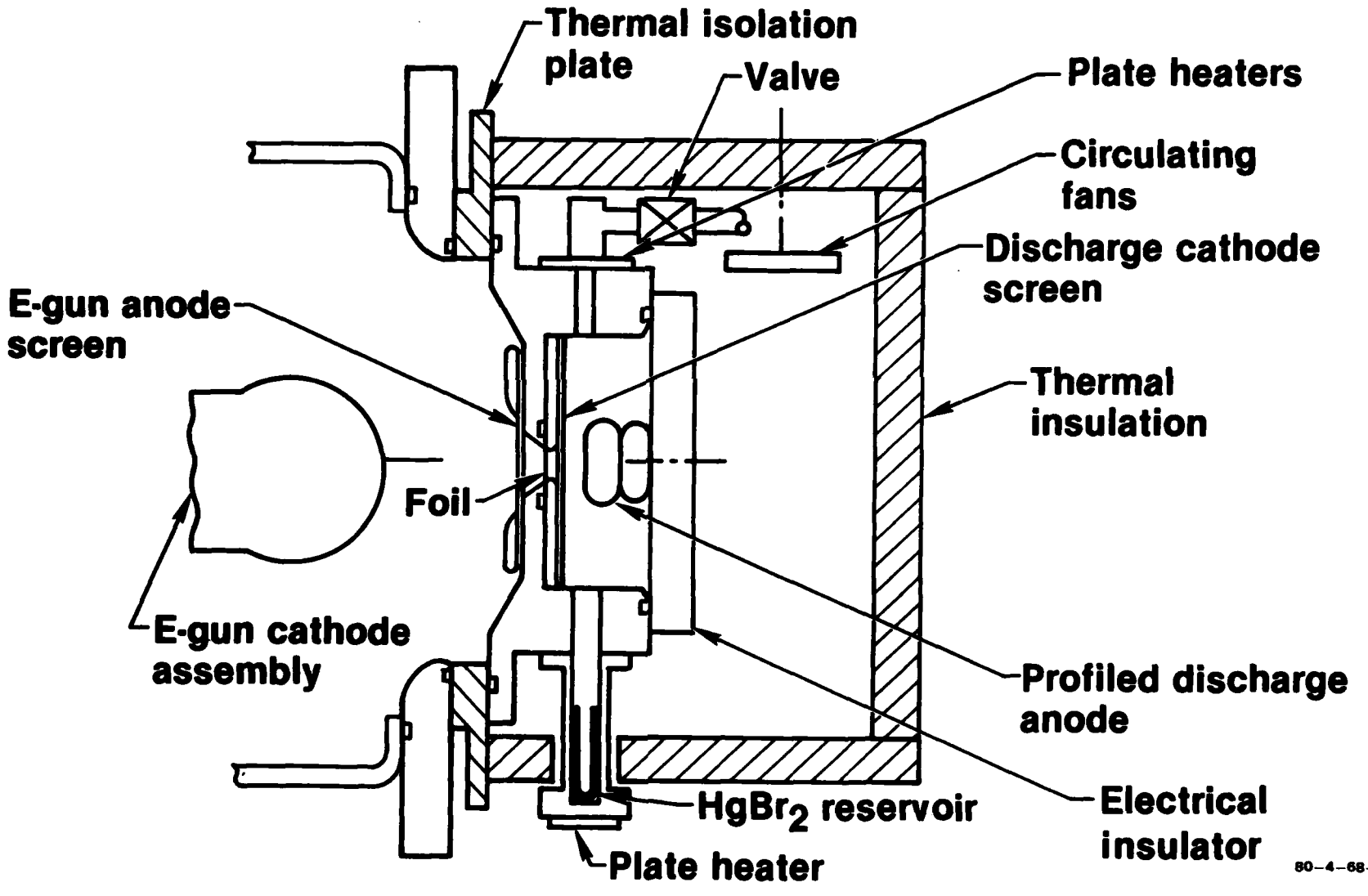
Thermal isolation plate
Valve
Plate heaters
Circulating fans
Discharge cathode screen
E-gun anode screen
Thermal insulation
Foil
E-gun cathode assembly
Profiled discharge anode
Electrical insulator
$HgBr_2$ reservoir
Plate heater
80-4-68-1

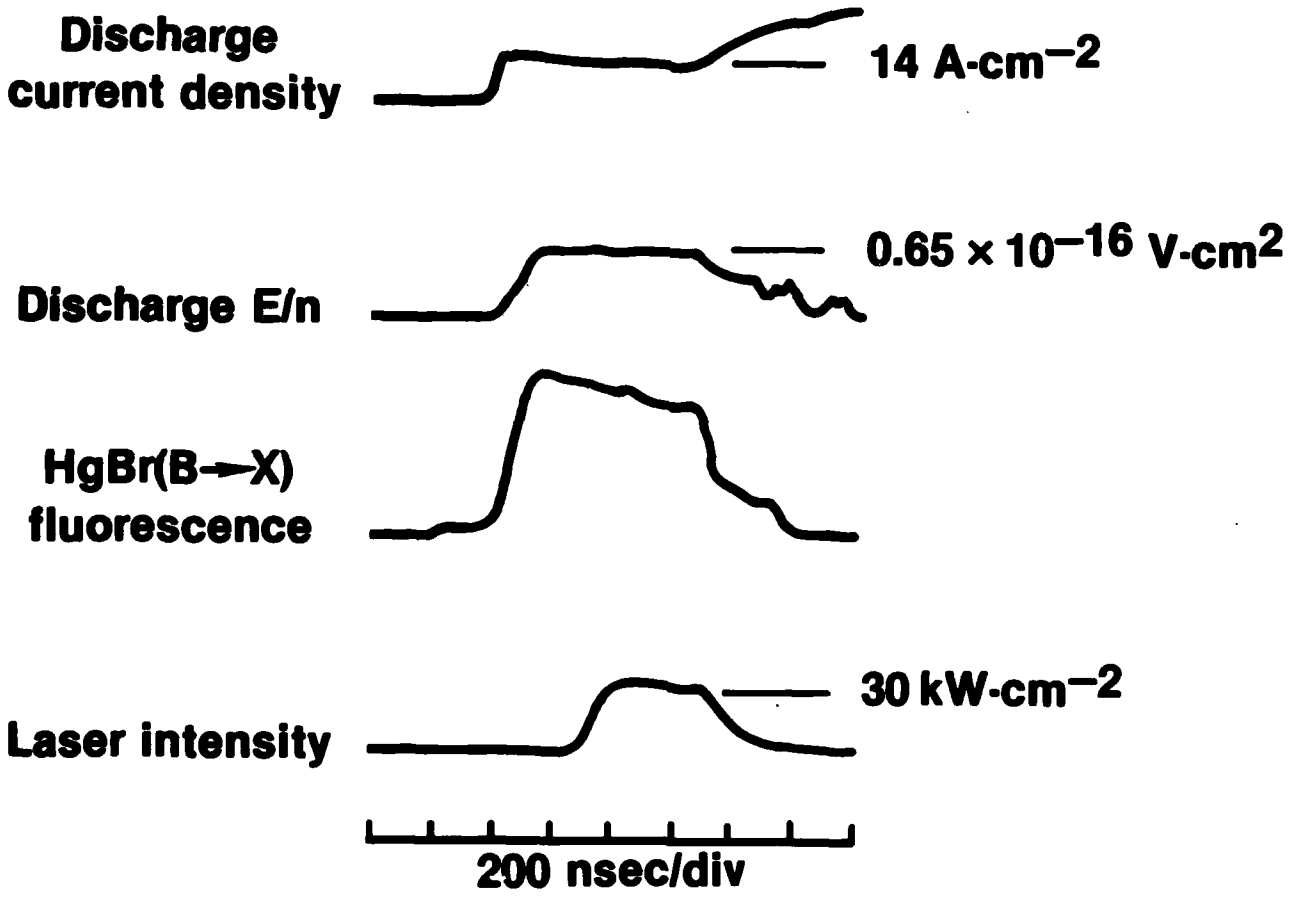
Discharge
current density
14 A-cm^{-2}
Discharge E/n
0.65 × 10^{-16} V-cm^2
HgBr(B→X)
fluorescence
Laser intensity
30 kW-cm^{-2}
200 nsec/div

80-7-45-1

June 1978

REPORTS DISTRIBUTION LIST FOR ONR PHYSICS PROGRAM OFFICE
UNCLASSIFIED CONTRACTS

Director Defense Advanced Research Projects Agency Attn: Technical Library 1400 Wilson Blvd. Arlington, Virginia 22209	3 copies
Office of Naval Research Physics Program Office (Code 421) 800 North Quincy Street Arlington, Virginia 22217	3 copies
Office of Naval Research Assistant Chief for Technology (Code 200) 800 North Quincy Street Arlington, Virginia 22217	1 copy
Naval Research Laboratory Department of the Navy Attn: Technical Library Washington, D. C. 20375	3 copies
Office of the Director of Defense Research and Engineering Information Office Library Branch The Pentagon Washington, D. C. 20301	3 copies
U. S. Army Research Office Box 12211 Research Triangle Park North Carolina 27709	2 copies
Defense Documentation Center Cameron Station (TC) Alexandria, Virginia 22314	12 copies
Director, National Bureau of Standards Attn; Technical Library Washington, DC 20234	1 copy
Commanding Officer Office of Naval Research Branch Office 536 South Clark Street Chicago, Illinois 60605	3 copies

Commanding Officer — 3 copies
Office of Naval Research Branch Office
1030 East Green Street
Pasadena, California 91101

San Francisco Area Office — 3 copies
Office of Naval Research
One Hallidie Plaza
Suite 601
San Francisco, California 94102

Commanding Officer — 3 copies
Office of Naval Research Branch Office
666 Summer Street
Boston, Massachusetts 02210

New York Area Office — 1 copy
Office of Naval Research
715 Broadway, 5th Floor
New York, New York 10003

Director — 1 copy
U. S. Army Engineering Research
and Development Laboratories
Attn: Technical Documents Center
Fort Belvoir, Virginia 22060

ODDR&E Advisory Group on Electron Devices — 3 copies
201 Varick Street
New York, New York 10014

Air Force Office of Scientific Research — 1 copy
Department of the Air Force
Bolling AFB, D. C. 22209

Air Force Weapons Laboratory — 1 copy
Technical Library
Kirtland Air Force Base
Albuquerque, New Mexico 87117

Air Force Avionics Laboratory — 1 copy
Air Force Systems Command
Technical Library
Wright-Patterson Air Force Base
Dayton, Ohio 45433

Lawrence Livermore Laboratory — 1 copy
Attn: Dr. W. F. Krupke
University of California
P. O. Box 808
Livermore, California 94550

Harry Diamond Laboratories — 1 copy
Technical Library
2800 Powder Mill Road
Adelphi, Maryland 20783

Naval Air Development Center — 1 copy
Attn: Technical Library
Johnsville
Warminster, Pennsylvania 18974

Naval Weapons Center — 1 copy
Technical Library (Code 753)
China Lake, California 93555

Naval Training Equipment Center — 1 copy
Technical Library
Orlando, Florida 32813

Naval Underwater Systems Center — 1 copy
Technical Library
New London, Connecticut 06320

Commandant of the Marine Corps — 1 copy
Scientific Advisor (Code RD-1)
Washington, DC 20380

Naval Ordnance Station — 1 copy
Technical Library
Indian Head, Maryland 20640

Naval Postgraduate School — 1 copy
Technical Library (Code 0212)
Monterey, California 93940

Naval Missile Center — 1 copy
Technical Library (Code 5632.2)
Point Mugu, California 93010

Naval Ordnance Station — 1 copy
Technical Library
Louisville, Kentucky 40214

Commanding Officer — 1 copy
Naval Ocean Research & Development Activity
Technical Library
NSTL Station, Mississippi 39529

Naval Explosive Ordnance Disposal Facility — 1 copy
Technical Library
Indian Head, Maryland 20640

Naval Ocean Systems Center — 1 copy
Technical Library
San Diego, California 92152

Naval Surface Weapons Center — 1 copy
Technical Library
Dahlgren, Virginia 22448

Naval Surface Weapons Center (White Oak) — 1 copy
Technical Library
Silver Spring, Maryland 20910

Naval Ship Research and Development Center — 1 copy
Central Library (Code L42 and L43)
Bethesda, Maryland 20084

Naval Avionics Facility — 1 copy
Technical Library
Indianapolis, Indiana 46218